

# Phenomenology of a Gauged $SU(3)^3$ Flavour Model

Andrzej J. Buras <sup>a,b)</sup>, Maria Valentina Carlucci <sup>a)</sup>,  
Luca Merlo <sup>a,b)</sup>, and Emmanuel Stamou <sup>a,b,c)</sup>

<sup>a)</sup> Physik-Department, Technische Universität München,  
James-Frank-Strasse, D-85748 Garching, Germany

<sup>b)</sup> TUM Institute for Advanced Study, Technische Universität München,  
Lichtenbergstrasse 2a, D-85748 Garching, Germany

<sup>c)</sup> Excellence Cluster Universe, Technische Universität München,  
Boltzmannstrasse 2, D-85748 Garching, Germany

*E-mail:* [andrzej.buras@ph.tum.de](mailto:andrzej.buras@ph.tum.de), [maria.carlucci@ph.tum.de](mailto:maria.carlucci@ph.tum.de),  
[luca.merlo@ph.tum.de](mailto:luca.merlo@ph.tum.de), [emmanuel.stamou@ph.tum.de](mailto:emmanuel.stamou@ph.tum.de)

## Abstract

We present an extensive analysis of  $\Delta F = 2$  observables and of  $B \rightarrow X_s \gamma$  in the framework of a specific Maximally Gauged Flavour (MGF) model of Grinstein *et al.* including all relevant contributions, in particular tree-level heavy gauge boson exchanges that are considered in the present paper for the first time. The model allows in principle for significant deviations from the Standard Model predictions for  $\varepsilon_K$ ,  $\Delta M_{B_{d,s}}$ , mixing induced  $CP$ -asymmetries  $S_{\psi K_S}$  and  $S_{\psi \phi}$  and  $B \rightarrow X_s \gamma$  decay. The tension between  $\varepsilon_K$  and  $S_{\psi K_S}$  present in the SM can be removed by enhancing  $|\varepsilon_K|$  without modifying  $S_{\psi K_S}$ . In this case, we find that in this model i) the results for  $S_{\psi \phi}$  and  $B \rightarrow X_s \gamma$  turn out to be SM-like, ii) the *exclusive determination* of  $|V_{ub}|$  is favoured and most importantly iii) the values of  $\Delta M_{B_d}$  and  $\Delta M_{B_s}$  being strongly correlated in this model with  $\varepsilon_K$  turn out to be much larger than the data for the central values of input parameters:  $\Delta M_{B_d} \approx 0.75/ps$  and  $\Delta M_{B_s} \approx 27/ps$ . Therefore, from the present perspective, the model suffers from a serious  $\varepsilon_K$ - $\Delta M_{B_{d,s}}$  tension. However, this tension can be softened considering theoretical and parametric uncertainties and in particular the decrease of the weak decay constants. On the other side, the model can be strongly constrained considering the theoretically cleaner ratios  $\Delta M_{B_d}/\Delta M_{B_s}$  and  $BR(B^+ \rightarrow \tau^+ \nu)/\Delta M_{B_d}$  and we find that it is unable to remove simultaneously all the SM tensions on the data. Finally, we compare the pattern of flavour violation in MGF with selected extensions of the SM.

# Contents

<b>1</b>	<b>Introduction</b>	<b>2</b>
<b>2</b>	<b>The Model</b>	<b>4</b>
<b>3</b>	<b><math>\Delta F = 2</math> Transitions</b>	<b>8</b>
3.1	Effective Hamiltonian . . . . .	8
3.2	Wilson Coefficients from Box-Diagrams . . . . .	9
3.3	Wilson Coefficients from Tree-Diagrams . . . . .	10
3.4	Properties . . . . .	11
3.5	QCD Corrections and Hadronic Matrix Elements . . . . .	12
3.6	Final Formulae for $\Delta F = 2$ Observables . . . . .	14
3.7	The Ratio $\Delta M_{B_d}/\Delta M_{B_s}$ and the $B^+ \rightarrow \tau^+ \nu$ Decay . . . . .	16
<b>4</b>	<b>The <math>b</math> semileptonic CP-asymmetry</b>	<b>16</b>
<b>5</b>	<b>The <math>\bar{B} \rightarrow X_s \gamma</math> Decay</b>	<b>17</b>
5.1	Effective Hamiltonian . . . . .	17
5.2	Contributions of $W$ -exchanges . . . . .	18
5.3	Contributions of $\hat{A}^m$ -exchanges . . . . .	19
<b>6</b>	<b>Numerical Analysis</b>	<b>19</b>
6.1	Anomalies in the Flavour Data . . . . .	19
6.1.1	The $\varepsilon_K - S_{\psi K_S}$ Anomaly . . . . .	19
6.1.2	The $ V_{ub} $ -Problem . . . . .	20
6.2	Input Parameters and the Parameter Space of the Model . . . . .	20
6.2.1	Input Parameters . . . . .	21
6.2.2	The CKM Matrix . . . . .	22
6.2.3	The Parameter Space of the Model . . . . .	23
6.3	Results . . . . .	23
6.3.1	Correlations Among the Observables . . . . .	26
<b>7</b>	<b>Comparison with other Models</b>	<b>30</b>
<b>8</b>	<b>Conclusion</b>	<b>31</b>
<b>A</b>	<b>Feynman Rules for MGF</b>	<b>33</b>
A.1	Couplings of SM Gauge and Goldstone bosons . . . . .	33
A.2	Couplings of Flavour Gauge Bosons . . . . .	34
<b>B</b>	<b>Couplings of the Lightest Flavour Gauge Boson</b>	<b>36</b>
	<b>References</b>	<b>39</b>

# 1 Introduction

The Standard Model (SM) of Particle Physics is successful in describing particles and their electroweak and strong interactions, still, several aspects are problematic. In this paper, we concentrate on the Flavour Problem.

The introduction of additional symmetries beyond the SM gauge group acting on the three fermion generations can produce realistic mass hierarchies and mixing textures. The Lagrangian is invariant under the gauge group of the SM and under the additional flavour symmetry at an energy scale equal or higher than the electroweak one. Fermion masses and mixings arise once these symmetries are broken, spontaneously or explicitly. Such flavour models differ from each other in the nature of the symmetries and the symmetry breaking mechanism. On the other hand, they all share the same top-down approach: the main goal is the explanation of fermion masses and mixings by the introduction of flavour symmetries; only as a second step their phenomenological consistency with FCNC processes (sometimes) is investigated (see Refs. [1, 2] and references therein).

A bottom-up approach consists in first identifying a low-energy effective scheme in which the contributions to FCNC observables are under control and subsequently in constructing high-energy models from which the effective description can be derived. The so-called Minimal Flavour Violation (MFV) [3, 4, 5, 6] follows this second approach. The fact that so far no evident deviations from the SM predictions have been found in any flavour process observed in the hadronic sector [7], from rare decays in the kaon and pion sector to  $B$  decays at super $B$ -factories, can be a sign that any physics beyond the SM does not introduce significant new sources of flavour and CP violation with respect to the SM. In Refs. [8, 9, 10, 11], this criterion has been rigorously defined in terms of flavour symmetries, considering an effective operator description within the SM. More in detail, restricted to the quark sector, the flavour symmetry coincides with the symmetry of the SM Lagrangian in the limit of vanishing Yukawa couplings. This symmetry can be written as the product of non-Abelian  $SU(3)$  terms,

$$G_f = SU(3)_{Q_L} \times SU(3)_{U_R} \times SU(3)_{D_R}, \quad (1.1)$$

and three additional  $U(1)$  factors, that can be arranged to correspond to the Baryon number, the Hypercharge and a phase transformation only on the right-handed (RH) down-type quarks. Interestingly, only the non-Abelian terms of  $G_f$  control the flavour structures of the quark mass-matrices, while the  $U(1)$  factors can only be responsible for overall suppressions [11]. The  $SU(2)_L$ -doublet  $Q_L$  and the  $SU(2)_L$ -singlets  $U_R$  and  $D_R$  transform under  $G_f$  as

$$Q_L \sim (\mathbf{3}, \mathbf{1}, \mathbf{1}), \quad U_R \sim (\mathbf{1}, \mathbf{3}, \mathbf{1}), \quad D_R \sim (\mathbf{1}, \mathbf{1}, \mathbf{3}). \quad (1.2)$$

In order to write the usual SM Yukawa terms,

$$\mathcal{L}_Y = \overline{Q}_L \mathcal{Y}_d D_R H + \overline{Q}_L \mathcal{Y}_u U_R \tilde{H} + \text{h.c.}, \quad (1.3)$$

where  $\tilde{H} = i\tau_2 H^*$ , manifestly invariant under  $G_f$ , the Yukawa couplings are promoted to dimensionless fields – called spurions – with non-trivial transformation properties under  $G_f$ :

$$\mathcal{Y}_u \sim (\mathbf{3}, \overline{\mathbf{3}}, \mathbf{1}), \quad \mathcal{Y}_d \sim (\mathbf{3}, \mathbf{1}, \overline{\mathbf{3}}). \quad (1.4)$$

Following the MFV ansatz, quark masses and mixings arise once the electroweak symmetry is spontaneously broken by the Higgs VEV,  $\langle H \rangle = v/\sqrt{2}$  with  $v = 246$  GeV, and the spurion fields obtain the values,

$$\mathcal{Y}_d = \frac{\sqrt{2}}{v} \begin{pmatrix} m_d & 0 & 0 \\ 0 & m_s & 0 \\ 0 & 0 & m_b \end{pmatrix} \quad \text{and} \quad \mathcal{Y}_u = \frac{\sqrt{2}}{v} \mathcal{V}^\dagger \begin{pmatrix} m_u & 0 & 0 \\ 0 & m_c & 0 \\ 0 & 0 & m_t \end{pmatrix}, \quad (1.5)$$

where  $\mathcal{V}$  is the unitary CKM matrix.

Recently, several papers [12, 13, 14] appeared where a MFV-like ansatz is implemented in the context of maximal gauge flavour (MGF) symmetries: in the limit of vanishing Yukawa interactions these gauge symmetries are the largest non-Abelian ones allowed by the Lagrangian of the model. The particle spectrum is enriched by new heavy gauge bosons, carrying neither colour nor electric charges, and exotic fermions, to cancel anomalies. Furthermore, the new exotic fermions give rise to the SM fermion masses through a See-Saw mechanism, in a way similar to how the light left-handed (LH) neutrinos obtain masses by the heavy RH ones. Moreover, the MFV spurions are promoted to scalar fields – called flavons – invariant under the gauge group of the SM, but transforming as bi-fundamental representations of the non-Abelian part of the flavour symmetry. Once the flavons develop suitable VEVs, the SM fermion masses and mixings are correctly described. Still, Refs. [12, 13, 14] do not provide a natural mechanism for the specific structure of the flavon VEVs (see Refs. [15, 16] for a recent discussion) and therefore a full analysis of the effects of such scalar fields is presently not possible.

Even if this approach has some similarities to the usual MFV description, the presence of flavour-violating neutral gauge bosons and exotic fermions introduces modifications of the SM couplings and tends to lead to dangerous contributions to FCNC processes mediated by the new heavy particles. Consequently, the MGF framework goes beyond the standard MFV and a full phenomenological analysis of this NP scenario is mandatory to judge whether it is consistent with all available data.

In this paper we focus on the specific MGF realisation presented in Ref. [12], even if our analysis can be easily applied to other models with gauge flavour symmetries. In particular, we extend the study performed in Ref. [12] and point out that the parameter space of such a model can be further constrained performing a full analysis on meson oscillations. Furthermore, we observe that the model, while solving the  $\varepsilon_K - S_{\psi K_S}$  tension, cannot simultaneously remove other SM flavour anomalies, which in some cases become even more pronounced.

Relative to Ref. [12] the new aspects of our analysis are:

- In addition to new box-diagram contributions to  $\Delta F = 2$  processes, considered already in Ref. [12], we include in our analysis tree-level exchanges of new heavy flavour gauge bosons. These diagrams generate LR operators that are strongly enhanced, by the renormalisation group (RG) QCD running, relatively to the standard LL operators and could a priori be very important.
- The impact of the new neutral current-current operators, arising from integrating out the heavy flavour gauge bosons, to the  $\bar{B} \rightarrow X_s \gamma$  has been studied in Ref. [17] and we apply those results to the model.



- We point out that this model favours a value of  $|V_{ub}|$  close to its determination from exclusive decays, i.e. in the ballpark of  $3.5 \times 10^{-3}$ . For slightly larger values, the model can still accommodate the considered observables within the errors, but for the inclusive determination of  $|V_{ub}|$  it suffers from tensions similar to the SM.
- We scan over all NP parameters and present a correlated analysis of  $\varepsilon_K$ , the mass differences  $\Delta M_{B_{d,s}}$  the  $B^+ \rightarrow \tau^+ \nu$  and  $\bar{B} \rightarrow X_s \gamma$  decays, the ratio  $\Delta M_{B_d}/\Delta M_{B_s}$ , the mixing-induced CP asymmetries  $S_{\psi K_S}$  and  $S_{\psi \phi}$ , and the  $b$  semileptonic CP-asymmetry  $A_{sl}^b$ .
- We find that large corrections to the CP observables in the meson oscillations,  $\varepsilon_K$ ,  $S_{\psi K_S}$  and  $S_{\psi \phi}$ , are allowed. However, requiring  $\varepsilon_K$  to stay inside its  $3\sigma$  error range, only small deviations from the SM values of  $S_{\psi K_S}$  and  $S_{\psi \phi}$  are allowed.
- We find that requiring  $\varepsilon_K$ - $S_{\psi K_S}$  tension to be removed in this model implies the values of  $\Delta M_{B_d}$  and  $\Delta M_{B_s}$  to be significantly larger than the data. While the inclusion of theoretical and parametric uncertainties and in particular the decrease of the weak decay constants could soften this problem, it appears from the present perspective that the model suffers from a serious  $\varepsilon_K - \Delta M_{B_{s,d}}$  tension.
- We also investigate the correlation among two theoretically cleaner observables,  $\Delta M_{B_d}/\Delta M_{B_s}$  and  $BR(B^+ \rightarrow \tau^+ \nu)/\Delta M_{B_d}$ . In this way, we strongly constrain the parameter space of the model and conclude that the tension in  $BR(B^+ \rightarrow \tau^+ \nu)$ , present already within the SM, is even increased.
- We compare the patterns of flavour violation in this model with those found in the original MFV, the MFV with the addition of flavour blind phases and MFV in the left-right asymmetric framework.
- As a by-product of our work we present a rather complete list of Feynman rules relevant for processes in the quark sector.

The structure of the paper is shown in the table of contents.

## 2 The Model

In this section we summarise the relevant features of the MGF construction presented in Ref. [12], dealing only with the quark sector. The flavour symmetry is that of eq. (1.1), but it is gauged. The spectrum is enriched by the corresponding flavour gauge bosons and by new exotic quarks, necessary to cancel the anomalies: in particular the new quarks are two coloured RH  $SU(3)_{Q_L}$ -triplets, one LH  $SU(3)_{U_R}$ -triplet and one LH  $SU(3)_{D_R}$ -triplet. In table 1, we list all the fields present in the theory and their transformation properties under the gauge groups.

With this matter content, the most general renormalisable Lagrangian invariant under the SM and flavour gauge groups can be divided into three parts:

$$\mathcal{L} = \mathcal{L}_{kin} + \mathcal{L}_{int} - V[H, Y_u, Y_d] . \quad (2.1)$$

	$Q_L$	$U_R$	$D_R$	$H$	$\Psi_{u_R}$	$\Psi_{d_R}$	$\Psi_{u_L}$	$\Psi_{d_L}$	$Y_u$	$Y_d$
$SU(3)_c$	<b>3</b>	<b>3</b>	<b>3</b>	<b>1</b>	<b>3</b>	<b>3</b>	<b>3</b>	<b>3</b>	<b>1</b>	<b>1</b>
$SU(2)_L$	<b>2</b>	<b>1</b>	<b>1</b>	<b>2</b>	<b>1</b>	<b>1</b>	<b>1</b>	<b>1</b>	<b>1</b>	<b>1</b>
$U(1)_Y$	$+1/6$	$+2/3$	$-1/3$	$+1/2$	$+2/3$	$-1/3$	$+2/3$	$-1/3$	0	0
$SU(3)_{Q_L}$	<b>3</b>	<b>1</b>	<b>1</b>	<b>1</b>	<b>3</b>	<b>3</b>	<b>1</b>	<b>1</b>	$\bar{\mathbf{3}}$	$\bar{\mathbf{3}}$
$SU(3)_{U_R}$	<b>1</b>	<b>3</b>	<b>1</b>	<b>1</b>	<b>1</b>	<b>1</b>	<b>3</b>	<b>1</b>	<b>3</b>	<b>1</b>
$SU(3)_{D_R}$	<b>1</b>	<b>1</b>	<b>3</b>	<b>1</b>	<b>1</b>	<b>1</b>	<b>1</b>	<b>3</b>	<b>1</b>	<b>3</b>

Table 1: *The transformation properties of the fields under the SM and flavour gauge symmetries.*

The first one,  $\mathcal{L}_{kin}$ , contains the kinetic terms of all the fields and the couplings of fermions and scalar bosons to the gauge bosons. The covariant derivative entering  $\mathcal{L}_{kin}$  accounts for SM gauge boson-fermion interactions and additional flavour interactions involving new gauge bosons and fermions:

$$D_\mu \supset \sum_{f=Q,U,D} i g_f N_f (A_f)_\mu, \quad (A_f)_\mu \equiv \sum_{a=1}^8 (A_f)_\mu \frac{\lambda_{SU(3)}^a}{2}, \quad (2.2)$$

where  $g_f$  are the flavour gauge coupling constants,  $N_f$  the quantum numbers,  $A_f^a$  the flavour gauge bosons and  $\lambda_{SU(3)}^a$  the Gell-Mann matrices.

The second term in eq. (2.1),  $\mathcal{L}_{int}$ , contains the quark mass terms and the quark-scalar interactions:

$$\begin{aligned} \mathcal{L}_{int} = & \lambda_u \bar{Q}_L \tilde{H} \Psi_{u_R} + \lambda'_u \bar{\Psi}_{u_L} Y_u \Psi_{u_R} + M_u \bar{\Psi}_{u_L} U_R + \\ & + \lambda_d \bar{Q}_L H \Psi_{d_R} + \lambda'_d \bar{\Psi}_{d_L} Y_d \Psi_{d_R} + M_d \bar{\Psi}_{d_L} D_R + \text{h.c.}, \end{aligned} \quad (2.3)$$

where  $M_{u,d}$  are universal mass parameters and  $\lambda_{u,d}^{(\prime)}$  are universal coupling constants that can be chosen real, through a redefinition of the fields.

The last term in eq. (2.1),  $V[H, Y_u, Y_d]$ , is the scalar potential of the model, containing the SM Higgs and the flavons  $Y_{u,d}$ . The mechanisms of both electroweak and flavour symmetry breaking arise from the minimisation of this scalar potential. It has not been explicitly constructed in Ref. [12] and it is beyond the scope of the present paper to provide such a scalar potential (see Ref. [16] for a recent analysis). Therefore, we assume that the spontaneous breaking of the electroweak symmetry proceeds as in the SM through the Higgs mechanism and that the spontaneous flavour symmetry breaking is driven by the flavon fields  $Y_{u,d}$  which develop the following VEVs:

$$\langle Y_d \rangle = \hat{Y}_d, \quad \langle Y_u \rangle = \hat{Y}_u V. \quad (2.4)$$

Here  $\hat{Y}_{u,d}$  are diagonal  $3 \times 3$  matrices and  $V$  is a unitary matrix. We emphasise that, despite the similarity to eq. (1.5) of MFV, the matrix  $V$  is not the CKM matrix and the vacuum expectation values  $\langle Y_{u,d} \rangle$  do not coincide with the SM Yukawa matrices. This is illustrated by moving to the fermion-mass eigenbasis. In what follows we focus on the up-quark sector, but analogous formulae can also be written for the down-quark sector. The LH and RH up-quarks mix separately giving rise to SM up-quarks  $u_{R,L}^i$  and exotic up-quarks  $u_{R,L}^{\prime i}$ :

$$\begin{pmatrix} u_{R,L}^i \\ u_{R,L}^{\prime i} \end{pmatrix} = \begin{pmatrix} c_{u(R,L)i} & -s_{u(R,L)i} \\ s_{u(R,L)i} & c_{u(R,L)i} \end{pmatrix} \begin{pmatrix} U_{R,L}^i \\ \Psi_{u_{R,L}}^i \end{pmatrix}, \quad (2.5)$$

where  $c_{u(R,L)i}$  and  $s_{u(R,L)i}$  are cosines and sines, respectively. Denoting with  $m_{fi}$  the mass of the up-type  $f^i = \{u^i, u^{\prime i}\}$  quark, what follows is a direct inverse proportionality between  $m_{u^i}$  and  $m_{u^{\prime i}}$ :

$$m_{u^i} m_{u^{\prime i}} = M_u \lambda_u \frac{v}{\sqrt{2}}. \quad (2.6)$$

We can express these masses in terms of the flavour symmetry breaking parameters:

$$m_{u^i} = \frac{s_{u_{Ri}} s_{u_{Li}}}{c_{u_{Ri}}^2 - s_{u_{Li}}^2} \lambda'_u (\hat{Y}_u)_i, \quad m_{u^{\prime i}} = \frac{c_{u_{Ri}} c_{u_{Li}}}{c_{u_{Ri}}^2 - s_{u_{Li}}^2} \lambda'_u (\hat{Y}_u)_i, \quad (2.7)$$

where a straightforward calculation gives

$$s_{u_{Li}} = \sqrt{\frac{m_{u^i}}{M_u} \left| \frac{\lambda_u v m_{u^{\prime i}} - \sqrt{2} M_u m_{u^i}}{\sqrt{2} (m_{u^{\prime i}}^2 - m_{u^i}^2)} \right|}, \quad s_{u_{Ri}} = \sqrt{\frac{m_{u^i}}{\lambda_u v} \left| \frac{\sqrt{2} M_u m_{u^{\prime i}} - \lambda_u v m_{u^i}}{m_{u^{\prime i}}^2 - m_{u^i}^2} \right|}. \quad (2.8)$$

These results are exact and valid for all quark generations. However, taking the limit  $m_{u^{\prime i}} \gg m_{u^i}$ , we find simple formulae that transparently expose the behaviour of the previous expressions. In this limit we find

$$m_{u^i} \approx \frac{v}{\sqrt{2}} \frac{\lambda_u M_u}{\lambda'_u (\hat{Y}_u)_i}, \quad m_{u^{\prime i}} \approx \lambda'_u (\hat{Y}_u)_i, \quad (2.9)$$

$$s_{u_{Li}} \approx \sqrt{\frac{m_{u^i}}{m_{u^{\prime i}}} \frac{\lambda_u v}{\sqrt{2} M_u}}, \quad s_{u_{Ri}} \approx \sqrt{\frac{m_{u^i}}{m_{u^{\prime i}}} \frac{\sqrt{2} M_u}{\lambda_u v}}, \quad (2.10)$$

as it is in the usual see-saw scheme in the limit of  $(\hat{Y}_u)_i \gg M_u, v$ . These simplified relations are valid for all the fermions, apart from the top-quark for which the condition  $m_{t'} \gg m_t$  is not satisfied and large corrections to eq. (2.10) are expected.

From eq. (2.10) we see that to reproduce the correct SM quark spectrum,  $\hat{Y}_u$  must have an inverted hierarchy with respect to the SM Yukawas.

The presence of new exotic quarks has a relevant impact on the SM couplings. Indeed, the charged current-current interactions including SM and heavy quarks are governed by a  $6 \times 6$  matrix which is constructed from the unitary  $3 \times 3$  matrix  $V$  of eq. (2.4) and the

$c_{u_{Li}}, c_{d_{Li}}, s_{u_{Li}}$  and  $s_{d_{Li}}$  with  $(i = 1, 2, 3)$  introduced above. Adopting a matrix notation, the non-unitary  $3 \times 3$  matrices

$$c_{u_L} V c_{d_L}, \quad s_{u_L} V s_{d_L} \quad (2.11)$$

describe the charged ( $W^+$ ) current-current interactions within the light and heavy systems, respectively. The analogous matrices

$$c_{u_L} V s_{d_L}, \quad s_{u_L} V c_{d_L} \quad (2.12)$$

describe the charged current-current interactions between light and heavy fermions. In this notation,  $c_{u,d_L}$  and  $s_{u,d_L}$  are diagonal matrices, whose entries are  $c_{u,d_{Li}}$  and  $s_{u,d_{Li}}$ , respectively. Moreover, we point out that in the no-mixing limit,  $c_{u,d_{Li}} \rightarrow 1$  and  $s_{u,d_{Li}} \rightarrow 0$ , the (non-unitary)  $6 \times 6$  matrix reduces to

$$\begin{pmatrix} V & 0 \\ 0 & 0 \end{pmatrix}. \quad (2.13)$$

In this case the CKM matrix coincides with the unitary matrix  $V$ . As soon as the mixing is switched on, the CKM is modified to include  $c_{u,d_L}$ , which breaks unitarity. However, these deviations from unitarity are quite small (see sec. 6.2.2). Moreover no new CP violating phases appear in the resulting CKM matrix. At first sight their absence implies no impact of new contributions to the CP-violating observables  $S_{\psi K_s}$  and  $S_{\psi\phi}$ . However, this is not the case due to the modification of the CKM matrix and the presence of flavour gauge bosons. In this respect, this framework does differ from the original MFV of Ref. [8].

A consequence of the modification of the CKM matrix is the breaking of the GIM mechanism if only SM quarks are considered in loop-induced processes. However, once also the exotic quarks are included the GIM mechanism is recovered. We return to this issue in sec. 3.4.

The interactions with the  $Z$  boson and the Higgs field are modified too. Their effects have been already discussed in Ref. [12] and it turned out that the largest constraint comes from the modified  $Z b \bar{b}$  coupling.

Once the flavour symmetry is spontaneously broken by the flavon VEVs, the flavour gauge bosons acquire masses and mix among themselves. Using the vector notation for the flavour gauge bosons,

$$\chi = (A_Q^1, \dots, A_Q^8, A_U^1, \dots, A_U^8, A_D^1, \dots, A_D^8)^T, \quad (2.14)$$

the corresponding mass Lagrangian reads

$$\mathcal{L}_{\text{mass}} = \frac{1}{2} \chi^T \mathcal{M}_A^2 \chi \quad \text{with} \quad \mathcal{M}_A^2 = \begin{pmatrix} M_{QQ}^2 & M_{QU}^2 & M_{QD}^2 \\ M_{UQ}^2 & M_{UU}^2 & 0 \\ M_{DQ}^2 & 0 & M_{DD}^2 \end{pmatrix}, \quad (2.15)$$

and

$$\begin{aligned}
(M_{QQ}^2)_{ab} &= \frac{1}{4} g_Q^2 \text{Tr} \left[ \langle Y_u \rangle \{ \lambda_{SU(3)}^a, \lambda_{SU(3)}^b \} \langle Y_u \rangle^\dagger + \langle Y_d \rangle \{ \lambda_{SU(3)}^a, \lambda_{SU(3)}^b \} \langle Y_d \rangle^\dagger \right] \\
(M_{UU}^2)_{ab} &= \frac{1}{4} g_U^2 \text{Tr} \left[ \langle Y_u \rangle \{ \lambda_{SU(3)}^a, \lambda_{SU(3)}^b \} \langle Y_u \rangle^\dagger \right] \\
(M_{DD}^2)_{ab} &= \frac{1}{4} g_D^2 \text{Tr} \left[ \langle Y_d \rangle \{ \lambda_{SU(3)}^a, \lambda_{SU(3)}^b \} \langle Y_d \rangle^\dagger \right] \\
(M_{QU}^2)_{ab} &= (M_{UQ}^2)_{ba} = -\frac{1}{2} g_Q g_U \text{Tr} \left[ \lambda_{SU(3)}^a \langle Y_u \rangle^\dagger \lambda_{SU(3)}^b \langle Y_u \rangle \right] \\
(M_{QD}^2)_{ab} &= (M_{DQ}^2)_{ba} = -\frac{1}{2} g_Q g_D \text{Tr} \left[ \lambda_{SU(3)}^a \langle Y_d \rangle^\dagger \lambda_{SU(3)}^b \langle Y_d \rangle \right].
\end{aligned} \tag{2.16}$$

In general, the diagonalisation of this mass-matrix is only numerically possible; for the rest of the paper we shall indicate with  $\hat{\mathcal{M}}_A^2$  the diagonal matrix of the gauge boson mass eigenstates  $\hat{A}^m$ , where  $m = 1, \dots, 24$ , and with  $\mathcal{W}(\hat{A}^m, A_f^a)$ , where  $f = \{Q, U, D\}$  and  $a = 1, \dots, 8$ , the transformation to move from the flavour-basis to the mass-basis (see App. A.2).

### 3 $\Delta F = 2$ Transitions

#### 3.1 Effective Hamiltonian

In the model in question the effective Hamiltonian for  $\Delta F = 2$  observables with external down-type quarks consists at the leading order in weak and flavour-gauge interactions of two parts:

- Box-diagrams with SM  $W$ -boson and up-type quark exchanges. Due to the mixing among light and heavy quarks, there are three different types of such diagrams: with light quarks only, with heavy quarks only or with both light and heavy quarks running in the box, as shown in Fig. 1. If only exchanges of SM quarks are considered,

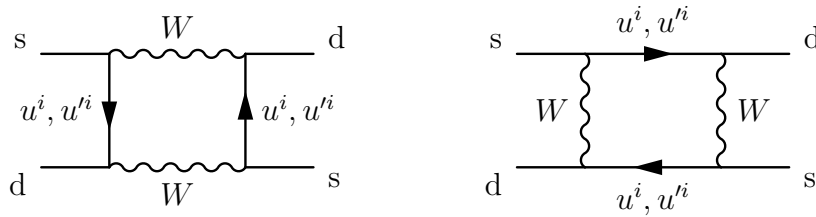


Figure 1: *The box-diagrams contributing to  $K^0 - \bar{K}^0$  mixing. Similarly for  $B_q^0 - \bar{B}_q^0$  mixing.*

the GIM mechanism is broken in these contributions. It is recovered when also the exchanges of heavy quarks are taken into account.

- The tree-level contributions from heavy gauge boson exchanges of Fig. 2, that generate new neutral current-current operators. These contributions clearly break the GIM mechanism.

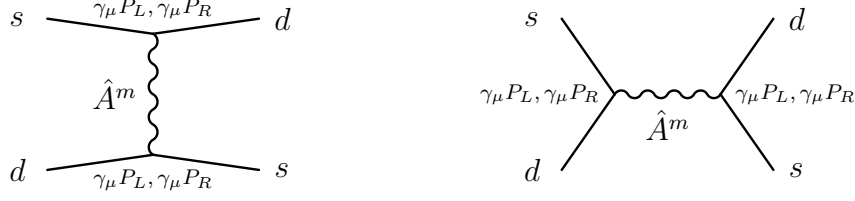


Figure 2: The tree-diagrams contributing to  $K^0 - \bar{K}^0$  mixing. Similarly, for  $B_q^0 - \bar{B}_q^0$  mixing.  $\hat{A}^m$  is a flavour gauge boson mass eigenstate.

In principle one could consider box-diagrams with flavour-violating neutral heavy boson exchanges but they are negligible with respect to the tree-level contributions.

The effective Hamiltonian for  $\Delta F = 2$  transitions can then be written in a general form as

$$\mathcal{H}_{\text{eff}}^{\Delta F=2} = \frac{G_F^2 M_W^2}{4\pi^2} \sum_{u^i} C_i(\mu) Q_i, \quad (3.1)$$

where  $M_W$  is the mass of the  $W$ -boson,  $Q_i$  are the relevant operators for the transitions, that we list below, and  $C_i(\mu)$  their Wilson coefficients evaluated at a scale  $\mu$ , which will be specified in the next section.

While in the SM only one operator contributes to each  $\Delta F = 2$  transition, i.e.  $Q_1^{\text{VLL}}(M)$  in the list of eq. (3.2), in the model in question there are more dimension-six operators. In the absence of flavon exchanges, the relevant operators for the  $M^0 - \bar{M}^0$  ( $M = K, B_d, B_s$ ) systems are [18]:

$$\begin{aligned} Q_1^{\text{VLL}}(K) &= (\bar{s}^\alpha \gamma_\mu P_L d^\alpha) (\bar{s}^\beta \gamma^\mu P_L d^\beta), & Q_1^{\text{VLL}}(B_q) &= (\bar{b}^\alpha \gamma_\mu P_L q^\alpha) (\bar{b}^\beta \gamma^\mu P_L q^\beta), \\ Q_1^{\text{VRR}}(K) &= (\bar{s}^\alpha \gamma_\mu P_R d^\alpha) (\bar{s}^\beta \gamma^\mu P_R d^\beta), & Q_1^{\text{VRR}}(B_q) &= (\bar{b}^\alpha \gamma_\mu P_R q^\alpha) (\bar{b}^\beta \gamma^\mu P_R q^\beta), \\ Q_1^{\text{LR}}(K) &= (\bar{s}^\alpha \gamma_\mu P_L d^\alpha) (\bar{s}^\beta \gamma^\mu P_R d^\beta), & Q_1^{\text{LR}}(B_q) &= (\bar{b}^\alpha \gamma_\mu P_L q^\alpha) (\bar{b}^\beta \gamma^\mu P_R q^\beta), \\ Q_2^{\text{LR}}(K) &= (\bar{s}^\alpha P_L d^\alpha) (\bar{s}^\beta P_R d^\beta), & Q_2^{\text{LR}}(B_q) &= (\bar{b}^\alpha P_L q^\alpha) (\bar{b}^\beta P_R q^\beta). \end{aligned} \quad (3.2)$$

where  $P_{L,R} = (1 \mp \gamma_5)/2$ .

In the next section, we collect the Wilson coefficients of these operators separating the contributions from box-diagrams and from the tree-level heavy gauge boson exchanges so that

$$C_i^{(M)} = \Delta_{\text{Box}}^{(M)} C_i + \Delta_{\text{A}}^{(M)} C_i, \quad (3.3)$$

where  $M = K, B_d, B_s$ .

### 3.2 Wilson Coefficients from Box-Diagrams

Keeping in mind the discussion around eqs. (2.11) and (2.12) we introduce the mixing parameters:

$$\lambda_i(K) = V_{is}^* V_{id}, \quad \lambda_i(B_q) = V_{ib}^* V_{iq}, \quad (3.4)$$

where  $q = d, s$  and  $V$  is not the CKM matrix but the unitary matrix of eq. (2.4).

Calculating the usual box-diagrams but including also contributions from heavy fermions (see Fig. 1) and corrections to  $W$ -quark vertices according to the Feynman rules in App. A.1 we find the following contributions to the Wilson coefficients relevant for the  $K^0 - \bar{K}^0$  system at the matching scale  $\mu_t$  in the ballpark of the top quark mass<sup>1</sup>:

$$\Delta_{\text{Box}}^{(K)} C_1^{VLL}(\mu_t) = \Delta_1(\mu_t, K) + \Delta_2(\mu_t, K) + \Delta_3(\mu_t, K), \quad (3.5)$$

where

$$\Delta_1(\mu_t, K) = (c_{d_{L1}} c_{d_{L2}})^2 \sum_{i,j=1,2,3} \lambda_i(K) \lambda_j(K) c_{u_{Li}}^2 c_{u_{Lj}}^2 F(x_i, x_j), \quad (3.6)$$

$$\Delta_2(\mu_t, K) = (c_{d_{L1}} c_{d_{L2}})^2 \sum_{i,j=1,2,3} \lambda_i(K) \lambda_j(K) s_{u_{Li}}^2 s_{u_{Lj}}^2 F(x'_i, x'_j), \quad (3.7)$$

$$\Delta_3(\mu_t, K) = (c_{d_{L1}} c_{d_{L2}})^2 \sum_{i,j=1,2,3} \lambda_i(K) \lambda_j(K) \left[ c_{u_{Li}}^2 s_{u_{Lj}}^2 F(x_i, x'_j) + s_{u_{Li}}^2 c_{u_{Lj}}^2 F(x'_i, x_j) \right]. \quad (3.8)$$

The arguments of the box-functions  $F$  are

$$x_i = \left( \frac{m_{u^i}}{M_W} \right)^2, \quad x'_j = \left( \frac{m_{u'^j}}{M_W} \right)^2, \quad (3.9)$$

where both  $i$  and  $j$  run over 1, 2, 3. The loop-function  $F(x_i, x_j)$  is

$$F(x_i, x_j) = \frac{1}{4} \left[ (4 + x_i x_j) I_2(x_i, x_j) - 8 x_i x_j I_1(x_i, x_j) \right] \quad (3.10)$$

with

$$\begin{aligned} I_1(x_i, x_j) &= \frac{1}{(1-x_i)(1-x_j)} + \left[ \frac{x_i \ln(x_i)}{(1-x_i)^2(x_i-x_j)} + (i \leftrightarrow j) \right], \\ I_2(x_i, x_j) &= \frac{1}{(1-x_i)(1-x_j)} + \left[ \frac{x_i^2 \ln(x_i)}{(1-x_i)^2(x_i-x_j)} + (i \leftrightarrow j) \right]. \end{aligned} \quad (3.11)$$

For the  $B_q^0 - \bar{B}_q^0$  mixing we have to replace  $K$  by  $B_q$  and  $c_{d_{L1}} c_{d_{L2}}$  by  $c_{d_{L1}} c_{d_{L3}}$  ( $c_{d_{L2}} c_{d_{L3}}$ ) in the case of  $q = d$  ( $q = s$ ). There are no contributions to other coefficients from box-diagrams.

### 3.3 Wilson Coefficients from Tree-Diagrams

Calculating the tree-level diagrams in Fig. 2 with the exchange of neutral gauge boson mass-eigenstates  $\hat{A}^m$  ( $m = 1, \dots, 24$ ) we find the following contributions to the Wilson coefficient at the high scale  $\mu_H$ , which is of the order of the mass of the corresponding

---

<sup>1</sup>We explain this choice in the context of QCD corrections below.



neutral gauge boson: for the  $K$  system we have

$$\Delta_A^{(K)} C_1^{VLL}(\mu_H) = \frac{4\pi^2}{G_F^2 M_W^2} \sum_{m=1}^{24} \frac{1}{2 \hat{M}_{A^m}^2} \left[ \left( \hat{\mathcal{G}}_L^d \right)_{ds,m} \right]^2 \quad (3.12)$$

$$\Delta_A^{(K)} C_1^{VRR}(\mu_H) = \frac{4\pi^2}{G_F^2 M_W^2} \sum_{m=1}^{24} \frac{1}{2 \hat{M}_{A^m}^2} \left[ \left( \hat{\mathcal{G}}_R^d \right)_{ds,m} \right]^2 \quad (3.13)$$

$$\Delta_A^{(K)} C_1^{LR}(\mu_H) = \frac{4\pi^2}{G_F^2 M_W^2} \sum_{m=1}^{24} \frac{1}{2 \hat{M}_{A^m}^2} \left[ 2 \left( \hat{\mathcal{G}}_L^d \right)_{ds,m} \left( \hat{\mathcal{G}}_R^d \right)_{ds,m} \right] \quad (3.14)$$

where the indices  $d$  and  $s$  stand for the external quarks  $d$  and  $s$ , while the index  $m$  refers to the  $\hat{A}^m$  gauge boson mass-eigenstate. The corresponding expressions for the  $B_d$  ( $B_s$ ) system are easily derived from the previous ones by substituting  $ds$  with  $db$  ( $sb$ ) in the indices of the couplings. The explicit expression for the couplings  $\left( \hat{\mathcal{G}}_{L,R}^d \right)_{ij,m}$  are given in App. A.2.

### 3.4 Properties

We note a few properties:

- Focussing on eqs. (3.6)–(3.8) and the corresponding expressions in the  $B_{d,s}$  systems, for a fixed  $\lambda_i \lambda_j$ , we have in the box-diagram contributions the combination

$$\mathcal{F}_{ij} \equiv c_{u_{Li}}^2 c_{u_{Lj}}^2 F(x_i, x_j) + s_{u_{Li}}^2 s_{u_{Lj}}^2 F(x'_i, x'_j) + c_{u_{Li}}^2 s_{u_{Lj}}^2 F(x_i, x'_j) + s_{u_{Li}}^2 c_{u_{Lj}}^2 F(x'_i, x_j). \quad (3.15)$$

If all fermion masses were degenerate, this combination would be independent of  $i, j$  and the unitarity of the matrix  $V$  would assure the vanishing of FCNC currents. This is precisely what one expects from the GIM mechanism.

- It is possible to arrange the function  $\mathcal{F}$  in order to match with the usual notation: for the  $K$  system we write

$$\begin{aligned} S_0(x_t) &\longrightarrow S_t^{(K)} \equiv (c_{d_{L1}} c_{d_{L2}})^2 (\mathcal{F}_{33} + \mathcal{F}_{11} - 2\mathcal{F}_{13}) , \\ S_0(x_c) &\longrightarrow S_c^{(K)} \equiv (c_{d_{L1}} c_{d_{L2}})^2 (\mathcal{F}_{22} + \mathcal{F}_{11} - 2\mathcal{F}_{12}) , \\ S_0(x_c, x_t) &\longrightarrow S_{ct}^{(K)} \equiv (c_{d_{L1}} c_{d_{L2}})^2 (\mathcal{F}_{23} + \mathcal{F}_{11} - \mathcal{F}_{13} - \mathcal{F}_{12}) . \end{aligned} \quad (3.16)$$

For the  $B_q$  systems we define similar functions  $S_i^{(B_q)}$  that can be simply derived from the previous ones by substituting  $c_{d_{L1}} c_{d_{L2}}$  with  $c_{d_{L1}} c_{d_{L3}}$  ( $c_{d_{L2}} c_{d_{L3}}$ ) in the case of  $q = d$  ( $q = s$ ). In particular the combination of the  $\mathcal{F}_{ij}$  factors are universal. In order to recover the  $S_0$  functions from the  $S_i^{(M)}$  expressions it is necessary to take the limit in which all the cosines are equal to 1 and all the sines are zero.

- The appearance of  $c_i$  and  $s_j$  factors introduces in general new flavour dependence, implying violation of certain MFV relations even in the absence of new CP-violating phases.

- There are no purely new CP-violating phases in this model, but the CP-odd phase of the CKM matrix induces sizeable new effects through new contributions to the mixing induced CP-asymmetries  $S_{\psi K_S}$  and  $S_{\psi\phi}$ , in the  $B_d^0 - \bar{B}_d$  and the  $B_s^0 - \bar{B}_s^0$  systems, respectively. Moreover, similarly to the mass differences  $\Delta M_{B_{d,s}}$ , new flavour-violating contributions affect the parameter  $\varepsilon_K$  and there are correlations between the new physics contributions to all these observables as we shall see below.
- The heavy flavour gauge bosons show flavour-violating couplings that can be strongly hierarchical: looking at the largest values of these couplings we find

$$\left(\hat{G}_{L,R}^d\right)_{sb} \gg \left(\hat{G}_{L,R}^d\right)_{db} \gg \left(\hat{G}_{L,R}^d\right)_{ds}, \quad \left(\hat{G}_{L,R}^u\right)_{ct} \gg \left(\hat{G}_{L,R}^u\right)_{ut} \gg \left(\hat{G}_{L,R}^u\right)_{uc}. \quad (3.17)$$

An example is presented in App. A.2 for the lightest gauge boson. This hierarchy is related to the sequential breaking of the flavour symmetry encoded in the flavon VEVs.

### 3.5 QCD Corrections and Hadronic Matrix Elements

The complete analysis requires the inclusion of the renormalisation group QCD evolution from the high scales, at which the initial effective Hamiltonians given above are constructed, down to low energy scales, at which the hadronic matrix elements are evaluated by lattice methods. A complication arises in the model in question as several rather different high scales are involved, such as the masses of the  $W$ -boson  $M_W$ , the masses of the neutral gauge bosons  $\hat{M}_{A^m}$  and the masses of heavy quarks  $m_{q^i}$ .

Before accounting for this problem we recall a very efficient method for the inclusion of all these QCD effects in the presence of a single high scale, which we denote by  $\mu_H$ . Instead of evaluating the hadronic matrix elements at the low-energy scale, we can evaluate them at  $\mu_H$ , corresponding to the scale at which heavy particles are integrated out. The amplitude for  $M - \bar{M}$  mixing ( $M = K^0, B_d^0, B_s^0$ ) at the scale  $\mu_H$  is then simply given by

$$\mathcal{A}(M \rightarrow \bar{M}) = \frac{G_F^2 M_W^2}{4\pi^2} \sum_{i,a} C_i^a(\mu_H) \langle \bar{M} | Q_i^a(\mu_H) | M \rangle, \quad (3.18)$$

where the sum runs over all the operators listed in eq. (3.2). The matrix element for  $M - \bar{M}$  mixing is given by

$$\langle \bar{M} | Q_i^a(\mu_H) | M \rangle = \frac{2}{3} m_M^2 F_M^2 P_i^a(M), \quad (3.19)$$

where the coefficients  $P_i^a(M)$  collect compactly all RG effects from scales below  $\mu_H$  as well as hadronic matrix elements obtained by lattice methods at low energy scales. Analytic formulae for all these coefficients,  $P_i^a(B_q)$  and  $P_i^a(K)$ , are given in Ref. [19], while the corresponding numerical values will be given below for some interesting values of  $\mu_H$ .

The question then is how to generalise this method to the case at hand which involves several rather different high scales. There are three types of contributions for which the relevant high energy scales attributed to the coefficients quoted above will differ from each other:

1. The SM box-diagrams involving  $W$ -bosons and the SM quarks. Here the scale is chosen to be  $\mu_t = \mathcal{O}(m_t)$ .
2. Tree-level diagrams mediated by neutral heavy gauge bosons,  $\hat{A}^m$ . Since we are taking into consideration the contributions from all such gauge bosons, we shall take as the initial scale for the RG evolution in each case exactly the mass of the involved gauge boson.
3. The only problematic case at first sight are the contributions from box-diagrams that involve simultaneously heavy and light particles. Here the correct procedure would be to integrate out first the heavy fermions and construct an effective field theory not involving them as dynamical degrees of freedom. However, as the only relevant contribution comes from the lightest exotic fermion<sup>2</sup>, that is  $t'$ , whose mass is relatively close to  $m_t$ , we can also here set the matching scale to be  $\mu_t$ . As the dominant effects from RG evolution, included here, come from scales below  $M_W$ , this procedure should sufficiently well approximate the exact one.

Having the initial conditions for Wilson coefficients at a given high scale  $\mu_H$  and provided also the corresponding hadronic matrix elements at this scale are known, we can calculate the relevant  $M - \bar{M}$  amplitude by means of eq. (3.18). As seen in eq. (3.19) these matrix elements are directly given in terms of the parameters  $P_i^a(K)$ ,  $P_i^a(B_d)$  and  $P_i^a(B_s)$  for which explicit expressions in terms of RG QCD factors and the non-perturbative parameters  $B_i^a(\mu_L)$  are given in eqs. (7.28)–(7.34) of Ref. [19]: the  $\mu_L$  denotes the low energy scale and it takes the value 2 GeV (4.6 GeV) for the  $K$  system ( $B_q$  systems).

The  $B_i^a(\mu_L)$  parameters are subject to considerable uncertainties. Exception are the  $B_1^{VLL}$  parameters for which a significant progress has been made in the recent years by lattice simulations. In the SM analysis, the RG invariant parameters  $\hat{B}_1^{VLL}$  are usually considered and denoted by  $\hat{B}_K$  and  $\hat{B}_{B_q}$ . We report their values in tab. 3. For completeness we recall the values of  $B_1^{VLL}$  that we extracted from the most recent lattice simulations:

$$\begin{aligned}
B_1^{VLL} &= 0.515(14), & \text{for } K \text{ system} \\
B_1^{VLL} &= 0.825(72), & \text{for } B_d \text{ system} \\
B_1^{VLL} &= 0.871(39), & \text{for } B_s \text{ system}.
\end{aligned} \tag{3.20}$$

As these parameters are the same for VRR contributions we will combine them together with the VLL contributions in the final formula at the end of this section.

Neglecting the unknown  $\mathcal{O}(\alpha_s)$  contributions to Wilson coefficients of the remaining operators at the high energy scale, our NLO RG analysis involves only the values of the coefficients  $P_1^{LR}(K)$ ,  $P_1^{LR}(B_d)$  and  $P_1^{LR}(B_s)$  calculated at  $\mu_H$ . To obtain these values we

---

<sup>2</sup>This is strictly true only for the  $B_q$  systems, because in the  $K$  system due to the CKM suppressions, the contribution from  $c'$  may be non-negligible. However, explicit computations confirmed that the most relevant contribution comes from  $t'$ .

need only the values of  $B_1^{LR}$  and  $B_2^{LR}$ , that we report below in the NDR scheme<sup>3</sup> [20, 21]:

$$\begin{aligned}
B_1^{LR} &= 0.562(39)(46), & B_2^{LR} &= 0.810(41)(31), & \text{for } K \text{ system} \\
B_1^{LR} &= 1.72(4)(^{+20}_{-6}), & B_2^{LR} &= 1.15(3)(^{+5}_{-7}), & \text{for } B_d \text{ system} \\
B_1^{LR} &= 1.75(3)(^{+21}_{-6}), & B_2^{LR} &= 1.16(2)(^{+5}_{-7}), & \text{for } B_s \text{ system}.
\end{aligned} \tag{3.21}$$

In tab. 2, we show the resulting  $P_i$  factors for some relevant values of  $\mu_H$ .

$\mu_H$	500 GeV	1 TeV	3 TeV	10 TeV
$P_1^{VLL}(\mu_H, K)$	0.392	0.384	0.373	0.363
$P_1^{LR}(\mu_H, K)$	-35.7	-39.3	-45.0	-51.4
$P_1^{VLL}(\mu_H, B_d)$	0.675	0.662	0.643	0.624
$P_1^{LR}(\mu_H, B_d)$	-2.76	-2.97	-3.31	-3.69
$P_1^{VLL}(\mu_H, B_s)$	0.713	0.698	0.678	0.659
$P_1^{LR}(\mu_H, B_s)$	-2.76	-2.97	-3.31	-3.69

Table 2: Central values of  $P_i$  factors for  $\mu_H = \{0.5, 1, 3, 10\}$  TeV.

Notice that the LR operators, arising from integrating out the heavy flavour gauge bosons, are strongly enhanced by the RG QCD running as can be deduced from the values of the  $P_1^{LR}$  factors. A priori, such contributions could be very important.

### 3.6 Final Formulae for $\Delta F = 2$ Observables

We collect here the formulae we shall use in our numerical analysis. The mixing amplitude  $M_{12}^i$  ( $i = K, d, s$ ) is related to the relevant effective Hamiltonian through

$$2 m_K (M_{12}^K)^* = \langle \bar{K}^0 | \mathcal{H}_{\text{eff}}^{\Delta S=2} | K^0 \rangle, \quad 2 m_{B_q} (M_{12}^q)^* = \langle \bar{B}_q^0 | \mathcal{H}_{\text{eff}}^{\Delta B=2} | B_q^0 \rangle \tag{3.22}$$

with  $q = d, s$ . The  $K_L - K_S$  mass difference and the CP-violating parameter  $\varepsilon_K$  are then given by

$$\Delta M_K = 2 \text{Re} (M_{12}^K), \quad \varepsilon_K = \frac{\kappa_\epsilon e^{i\varphi_\epsilon}}{\sqrt{2}(\Delta M_K)_{\text{exp}}} \text{Im} (M_{12}^K), \tag{3.23}$$

where  $\varphi_\epsilon = (43.51 \pm 0.05)^\circ$  and  $\kappa_\epsilon = 0.94 \pm 0.02$  takes into account that  $\varphi_\epsilon \neq \pi/4$  and includes long distance effect in  $\text{Im} \Gamma_{12}$  [22] and  $\text{Im} M_{12}$  [23]. The mixing amplitude entering the previous expressions can be decomposed into two parts, one containing the  $LL$  and  $RR$  contributions and the second only the  $LR$  ones:

$$M_{12}^K = (M_{12}^K)_1 + (M_{12}^K)_2, \tag{3.24}$$

---

<sup>3</sup>These values can be found in Refs. [20, 21], where  $B_1^{LR}$  ( $B_2^{LR}$ ) is called  $B_5$  ( $B_4$ ).

where

$$\begin{aligned}
(M_{12}^K)_1 &= \frac{G_F^2 M_W^2}{12\pi^2} F_K^2 m_K \left[ \hat{B}_K \eta_1 \lambda_2^2(K) S_c^{(K)} + \hat{B}_K \eta_2 \lambda_3^2(K) S_t^{(K)} + \right. \\
&\quad \left. + 2 \hat{B}_K \eta_3 \lambda_2(K) \lambda_3(K) S_{ct}^{(K)} + \right. \\
&\quad \left. + P_1^{VLL}(\mu_H, K) \left( \Delta_A^{(K)} C_1^{VLL}(\mu_H) + \Delta_A^{(K)} C^{VRR}(\mu_H) \right) \right]^*, \\
(M_{12}^K)_2 &= \frac{G_F^2 M_W^2}{12\pi^2} F_K^2 m_K P_1^{LR}(\mu_H, K) \Delta_A^{(K)} C_1^{LR*}(\mu_H).
\end{aligned} \tag{3.25}$$

Analogously, for the the  $B_{d,s}^0 - \bar{B}_{d,s}^0$  systems the two parts of the mixing amplitude are given by:

$$\begin{aligned}
(M_{12}^q)_1 &= \frac{G_F^2 M_W^2}{12\pi^2} F_{B_q}^2 m_{B_q} \left[ \eta_B \hat{B}_{B_q} \lambda_3^2(B_q) S_t^{(B_q)} + \right. \\
&\quad \left. + P_1^{VLL}(\mu_H, B_q) \left( \Delta_A^{(B_q)} C_1^{VLL}(\mu_H) + \Delta_A^{(B_q)} C^{VRR}(\mu_H) \right) \right]^*, \\
(M_{12}^q)_2 &= \frac{G_F^2 M_W^2}{12\pi^2} F_{B_q}^2 m_{B_q} P_1^{LR}(\mu_H, B_q) \Delta_A^{(B_q)} C_1^{LR*}(\mu_H).
\end{aligned} \tag{3.26}$$

Here  $\eta_{1,2,3,B}$  are known SM QCD corrections given in tab. 3 and  $P_i^a(\mu_H, M)$  describe the QCD evolution from  $\mu_H$  down to  $\mu_L$  for the considered system. For the  $B_q$  systems, it is useful to rearrange the definition of the mixing amplitude  $M_{12}^q$  as follows [24]

$$M_{12}^q = (M_{12}^q)_{\text{SM}} C_{B_q} e^{2i\varphi_{B_q}}, \tag{3.27}$$

where  $C_{B_{d,s}}$  and  $\varphi_{B_{d,s}}$  account for deviations from the SM contributions. Therefore, the mass differences turn out to be

$$\Delta M_{B_q} = 2 |M_{12}^q| = (\Delta M_{B_q})_{\text{SM}} C_{B_q} \quad (q = d, s), \tag{3.28}$$

where

$$(M_{12}^d)_{\text{SM}} = |(M_{12}^d)_{\text{SM}}| e^{2i\beta}, \quad (M_{12}^s)_{\text{SM}} = |(M_{12}^s)_{\text{SM}}| e^{2i\beta_s}. \tag{3.29}$$

Here the phases  $\beta \approx 22^\circ$  and  $\beta_s \simeq -1^\circ$  are defined through

$$V_{td}^{SM} = |V_{td}^{SM}| e^{-i\beta} \quad \text{and} \quad V_{ts}^{SM} = -|V_{ts}^{SM}| e^{-i\beta_s}. \tag{3.30}$$

The coefficients of  $\sin(\Delta M_{B_d} t)$  and  $\sin(\Delta M_{B_s} t)$  in the time dependent asymmetries in  $B_d^0 \rightarrow \psi K_S$  and  $B_s^0 \rightarrow \psi \phi$  are then given, respectively, by:

$$S_{\psi K_S} = \sin(2\beta + 2\varphi_{B_d}), \quad S_{\psi \phi} = \sin(2|\beta_s| - 2\varphi_{B_s}). \tag{3.31}$$

Notice that in the presence of non-vanishing  $\varphi_{B_d}$  and  $\varphi_{B_s}$  these two asymmetries do not measure  $\beta$  and  $\beta_s$  but  $(\beta + \varphi_{B_d})$  and  $(|\beta_s| - \varphi_{B_s})$ , respectively.

### 3.7 The Ratio $\Delta M_{B_d}/\Delta M_{B_s}$ and the $B^+ \rightarrow \tau^+ \nu$ Decay

The expressions for the mass-differences recovered in the previous section are affected by large uncertainties, driven by the decay constants  $F_{B_{d,s}}$ . To soften the dependence of our analysis on these theoretical errors, we consider the ratio among  $\Delta M_{B_d}$  and  $\Delta M_{B_s}$ , that we call  $R_{\Delta M_B}$ , and the ratio among the branching ratio of the  $B^+ \rightarrow \tau^+ \nu$  decay and  $\Delta M_{B_d}$ , that we name  $R_{BR/\Delta M}$ .

Indeed, when considering  $R_{\Delta M_B}$ , we notice that the SM theoretical errors are encoded into the parameter  $\xi = 1.237 \pm 0.032$ , that is much less affected by uncertainties with respect to the mass differences. When considering the NP effects, we obtain

$$R_{\Delta M_B} = \frac{(\Delta M_{B_d})_{\text{SM}} C_{B_d}}{(\Delta M_{B_s})_{\text{SM}} C_{B_s}}. \quad (3.32)$$

On the other hand, in the SM, the  $B^+ \rightarrow \tau^+ \nu$  decay occurs at the tree-level through the exchange of the  $W$ -boson. Therefore, the expression for its branching ratio is only slightly modified in our model:

$$BR(B^+ \rightarrow \tau^+ \nu) = \frac{G_F^2 m_{B^+} m_\tau^2}{8\pi} \left(1 - \frac{m_\tau^2}{m_{B^+}^2}\right)^2 F_{B^+}^2 |c_{uL1} V_{ub} c_{dL3}|^2 \tau_{B^+}, \quad (3.33)$$

where the NP effects are represented by the cosines. Notice that heavy flavour gauge boson contributions could contribute only at the loop-level and can be safely neglected, since they compete with a tree-level process. Furthermore, in the previous expression we have assumed the SM couplings for the leptons to the  $W$ -boson: even if we are not considering the lepton sector in our analysis it is reasonable to assume that any NP modification can be safely negligible, as these couplings are strongly constrained by the SM electroweak analysis.

In the ratio  $R_{BR/\Delta M}$ , the dependence on  $F_{B_d}$ , which is indeed the main source of the theoretical error on  $\Delta M_{B_d}$ , is cancelled [25, 26]:

$$R_{BR/\Delta M} = \frac{3\pi \tau_{B^+}}{4\eta_B \hat{B}_{B_d} S_0(x_t)} \frac{c_{uL1}^2 c_{dL3}^2 m_\tau^2}{C_{B_d} M_W^2} \frac{|V_{ub}|^2}{|V_{tb}^* V_{td}|^2} \left(1 - \frac{m_\tau^2}{m_{B_d}^2}\right)^2, \quad (3.34)$$

where the second fraction contains all NP contributions and we took  $m_{B^+} \approx m_{B_d}$ , well justified considering the errors in the other quantities. The SM prediction of this observable should be compared with the data

$$R_{BR/\Delta M} = (3.25 \pm 0.67) \times 10^{-4} \text{ ps}. \quad (3.35)$$

See tab. 4 for the SM prediction.

## 4 The $b$ semileptonic CP-asymmetry

In the  $B_q$  systems, apart from  $\Delta M_{B_q}$ ,  $S_{\psi K_S}$  and  $S_{\psi\phi}$ , a third quantity providing information on the meson mixings is the  $b$  semileptonic CP-asymmetry  $A_{sl}^b$  [27, 28]:

$$A_{sl}^b = (0.594 \pm 0.022) a_{sl}^d + (0.406 \pm 0.022) a_{sl}^s, \quad (4.1)$$

where

$$\begin{aligned} a_{sl}^d &= \left| \frac{(\Gamma_{12}^d)_{SM}}{(M_{12}^d)_{SM}} \right| \sin \phi_d = (5.4 \pm 1.0) \times 10^{-3} \sin \phi_d, \\ a_{sl}^s &= \left| \frac{(\Gamma_{12}^s)_{SM}}{(M_{12}^s)_{SM}} \right| \sin \phi_s = (5.0 \pm 1.1) \times 10^{-3} \sin \phi_s, \end{aligned} \quad (4.2)$$

with

$$\begin{aligned} \phi_d &= \arg \left( - (M_{12}^d)_{SM} / (\Gamma_{12}^d)_{SM} \right) = -4.3^\circ \pm 1.4^\circ, \\ \phi_s &= \arg \left( - (M_{12}^s)_{SM} / (\Gamma_{12}^s)_{SM} \right) = 0.22^\circ \pm 0.06^\circ. \end{aligned} \quad (4.3)$$

In the presence of NP, these expressions are modified. Since we have already discussed the NP effects on  $M_{12}^q$  in the previous sections, we focus now only on  $\Gamma_{12}^q$ . It is useful to adopt a notation for  $\Gamma_{12}^q$  similar to the one in eq. (3.27) for  $M_{12}^q$ :

$$\Gamma_{12}^q = (\Gamma_{12}^q)_{SM} \tilde{C}_{B_q} e^{-2i\tilde{\varphi}_{B_q}}, \quad (4.4)$$

where  $\tilde{C}_{B_q}$  is a real parameter. With such a notation we get,

$$a_{sl}^q = \left| \frac{(\Gamma_{12}^d)_{SM}}{(M_{12}^d)_{SM}} \right| \frac{\tilde{C}_{B_q}}{C_{B_q}} \sin(\phi_d + 2\varphi_{B_q} + 2\tilde{\varphi}_{B_q}). \quad (4.5)$$

Notice, that in the MGF context we are considering, the phase  $\tilde{\varphi}_{B_q}$  is vanishing, while  $\tilde{C}_{B_q}$  is mainly given by  $c_{uL2}^2 c_{dLb} c_{dLq} \approx 1$ . As a result the only NP modifications are provided by the NP contributions on  $M_{12}^q$ .

## 5 The $\bar{B} \rightarrow X_s \gamma$ Decay

### 5.1 Effective Hamiltonian

The decay  $\bar{B} \rightarrow X_s \gamma$  is mediated by the photonic dipole operators  $Q_{7\gamma}$  and  $Q'_{7\gamma}$  and through mixing also by the gluonic dipole operators  $Q_{8G}$  and  $Q'_{8G}$ . In our conventions they read

$$\begin{aligned} Q_{7\gamma} &= \frac{e}{16\pi^2} m_b \bar{s}_\alpha \sigma^{\mu\nu} P_R b_\alpha F_{\mu\nu}, \\ Q_{8G} &= \frac{g_s}{16\pi^2} m_b \bar{s}_\alpha \sigma^{\mu\nu} P_R T_{\alpha\beta}^a b_\beta G_{\mu\nu}^a \end{aligned} \quad (5.1)$$

and the corresponding primed dipole operators are obtained by substituting  $P_R$  with  $P_L$ .

The effective Hamiltonian for  $b \rightarrow s \gamma$  at a scale  $\mu$  in the SM normalisation and considering only the dipole operators reads

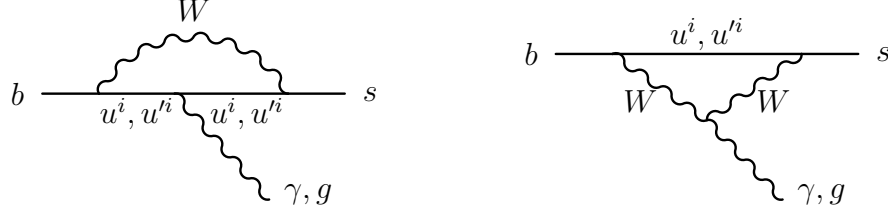
$$\begin{aligned} \mathcal{H}_{\text{eff}}^{b \rightarrow s \gamma} &= -\frac{4G_F}{\sqrt{2}} V_{ts}^* V_{tb} \left[ \Delta C_{7\gamma}(\mu) Q_{7\gamma} + \Delta C_{8G}(\mu) Q_{8G} + \right. \\ &\quad \left. + \Delta C'_{7\gamma}(\mu) Q'_{7\gamma} + \Delta C'_{8G}(\mu) Q'_{8G} \right]. \end{aligned} \quad (5.2)$$



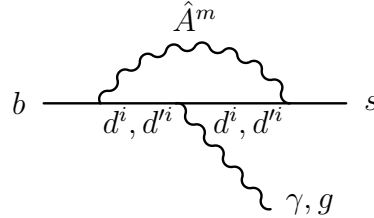
We have kept the contributions of the primed dipole operators  $Q'_{7\gamma}$  and  $Q'_{8G}$  even though their Wilson coefficients are suppressed by  $m_s/m_b$  with respect to the unprimed Wilson coefficients. However, the mixing of neutral current-current operators into  $Q'_{7\gamma}$  and  $Q'_{8G}$  can affect  $\Delta C'_{7\gamma}(\mu_b)$  as shown in Ref. [17].

Similarly to the Hamiltonian for the  $\Delta F = 2$  transitions, the Wilson coefficients in the Hamiltonian can be separated into two parts:

- The SM-like contribution from diagrams with  $W$ -bosons with modified couplings to both SM and exotic quarks of charge  $+2/3$ , denoted below by  $u$  and  $u'$ , respectively:



- The contribution of heavy neutral gauge bosons exchanges with virtual SM and exotic quarks of charge  $-1/3$ , denoted below by  $d$  and  $d'$ , respectively:



The first contribution has already been considered in Ref. [12], while the second, the impact of the heavy neutral gauge bosons on  $b \rightarrow s\gamma$ , has been recently pointed out in Ref. [17]. In particular it has been found that the QCD renormalisation group effects in the neutral gauge boson contributions can strongly affect the branching ratio of  $\bar{B} \rightarrow X_s\gamma$  and cannot be neglected a priori.

## 5.2 Contributions of $W$ -exchanges

For the  $W$ -exchange the matching is performed at the EW scale,  $\mu_W$ . The Wilson coefficients are the sum of  $t$  and  $t'$  contribution, since  $c'$  and  $u'$  contributions are suppressed by their small couplings to  $b$  and  $s$  quarks. Hence, the Wilson coefficients of  $Q_{7\gamma}$  and  $Q_{8G}$  are

$$\Delta_W C_{7\gamma}(\mu_W) = c_{d_{L2}} c_{d_{L3}} (c_{u_{L3}}^2 C_{7\gamma}^{SM}(x_t) + s_{u_{L3}}^2 C_{7\gamma}^{SM}(x'_t)) , \quad (5.3)$$

$$\Delta_W C_{8G}(\mu_W) = c_{d_{L2}} c_{d_{L3}} (c_{u_{L3}}^2 C_{8G}^{SM}(x_t) + s_{u_{L3}}^2 C_{8G}^{SM}(x'_t)) , \quad (5.4)$$

with

$$C_{7\gamma}^{SM}(x) = \frac{3x^3 - 2x^2}{4(x-1)^4} \ln x - \frac{8x^3 + 5x^2 - 7x}{24(x-1)^3} , \quad (5.5)$$

$$C_{8G}^{SM}(x) = \frac{-3x^2}{4(x-1)^4} \ln x - \frac{x^3 - 5x^2 - 2x}{8(x-1)^3} \quad (5.6)$$

being the SM Inami-Lim functions [29].

At last we need to evolve  $\Delta_W C(\mu_W)$  down to  $\mu_b$  to obtain the contribution of  $W$  exchanges to the branching ratio of  $\bar{B} \rightarrow X_s \gamma$ . The QCD analysis, that involves the SM charged current-current operators  $Q_1$  and  $Q_2$  as well as the QCD-penguins  $Q_3$  to  $Q_6$ , which mix with  $Q_{7\gamma}$  and  $Q_{8G}$  below  $\mu_t$ , is the same as in the SM and we proceed as in Ref. [17].

### 5.3 Contributions of $\hat{A}^m$ -exchanges

The contribution of a neutral gauge boson to the effective Hamiltonian in eq. (5.2) derives from integrating out the mass-eigenstate of the heavy flavour gauge boson  $\hat{A}^m$  at its mass-scale  $\mu_H$ . The Wilson coefficients  $\Delta_A C_{7\gamma}^{(\prime)}(\mu_H)$  and  $\Delta_A C_{8G}^{(\prime)}(\mu_H)$  have been calculated within a generic framework in Ref. [17]. The results for the special MGF case we are discussing are fixed by the couplings of the flavour gauge bosons to both SM and exotic fermions. Applying general formulae of Ref. [17] to the present case we found that these contributions are below 1% and can be safely neglected. As discussed in Ref. [17] the reason for such suppression are the See-saw-like couplings of flavour gauge bosons to both SM and exotic fermions and the heavy neutral gauge boson masses.

## 6 Numerical Analysis

Having at hand the analytic expressions derived in the previous sections, we are ready to perform a numerical analysis of the MGF model in question.

The first question we ask is whether the model is able to remove various anomalies in the flavour data hinting the presence of NP. Since the number of parameters is much smaller than in other popular extensions of the SM like SUSY models, LHT model, RS-scenario and models with left-right symmetry, it is indeed not obvious that these anomalies can be removed or at least softened. We briefly review the flavour anomalies as seen from the SM point of view.

### 6.1 Anomalies in the Flavour Data

#### 6.1.1 The $\varepsilon_K - S_{\psi K_S}$ Anomaly

It has been pointed out in Refs. [30, 22, 31, 32] that the SM prediction for  $\varepsilon_K$  implied by the measured value of  $S_{\psi K_S} = \sin 2\beta$ , the ratio  $R_{\Delta M_B}$ , and the value of  $|V_{cb}|$  is too small to agree well with the experiment. We obtain the SM  $\varepsilon_K$  value by taking the experimental value of  $S_{\psi K_S}$ , the ultimate  $|V_{cb}|$  determination, the most recent value of the non-perturbative parameter  $\hat{B}_K$  [33, 34, 35, 36, 37, 38], and by including long-distance effects in  $\text{Im}\Gamma_{12}$  [22] and  $\text{Im}M_{12}$  [23] as well as recently calculated NNLO QCD corrections to  $\varepsilon_K$  [39, 40]. We find<sup>4</sup>  $|\varepsilon_K| = (1.82 \pm 0.28) \times 10^{-3}$ , visibly below the experimental value.

On the other hand  $\sin 2\beta = 0.85 \pm 0.05$  from SM fits of the Unitarity Triangle is significantly larger than the experimental value. This discrepancy is to some extent caused by the desire to fit both  $\varepsilon_K$  [30, 22, 31] and  $BR(B^+ \rightarrow \tau^+ \nu)$  [41].

---

<sup>4</sup>The small discrepancy with respect to the value of Ref. [40] comes solely from updated input values.

As demonstrated in [22, 31], whether the NP is required in  $\varepsilon_K$  or  $S_{\psi K_S}$  depends on the values of  $\gamma$ ,  $|V_{ub}|$  and  $|V_{cb}|$ . The phase  $\gamma$  should be measured precisely by LHCb in the coming years while  $|V_{ub}|$  and  $|V_{cb}|$  should be precisely determined by Belle II and Super- $B$  provided that also the hadronic uncertainties will be under a better control.

### 6.1.2 The $|V_{ub}|$ -Problem

There is a tension between inclusive and exclusive determinations of  $|V_{ub}|$ . This means that if we take the unitarity of the CKM matrix as granted and also consider the good agreement of the ratio  $R_{\Delta M_B}$  with the data, the inclusive and exclusive determinations imply different patterns of NP in CP-violating observables. Indeed one is lead to consider two limiting scenarios:

**Scenario 1: Small  $|V_{ub}|$ .** Here  $|V_{ub}|$  is in principle the exclusive determination,

$$|V_{ub}| = (3.38 \pm 0.36) \times 10^{-3}. \quad (6.1)$$

Within the SM, when the  $\Delta M_{B_s}/\Delta M_{B_d}$  constraint is taken into account, one finds  $S_{\psi K_S} \approx 0.67$  in agreement with the data, but  $\varepsilon_K \approx 1.8 \times 10^{-3}$  visibly below the data. As discussed in Refs. [22, 31], a sizeable constructive NP contribution to  $\varepsilon_K$  would not require an increased value of  $\sin 2\beta$  relative to the experimental value of  $S_{\psi K_S}$ . NP of this type would then remove the  $\varepsilon_K - S_{\psi K_S}$  anomaly in the presence of the exclusive value of  $|V_{ub}|$ .

**Scenario 2: Large  $|V_{ub}|$ .** In this case  $|V_{ub}|$  corresponds to its inclusive determination,

$$|V_{ub}| = (4.27 \pm 0.38) \times 10^{-3}. \quad (6.2)$$

In this scenario the SM predicts  $\varepsilon_K \approx 2.2 \times 10^{-3}$ , in agreement with the data, while  $S_{\psi K_S} \approx 0.81$  is significantly above the data. As discussed in Refs. [30, 22], a negative NP phase  $\varphi_{B_d}$  in  $B_d^0 - \bar{B}_d^0$  mixing would solve the  $\varepsilon_K - S_{\psi K_S}$  anomaly in this case (see eq. (3.31)), provided such a phase is phenomenologically allowed by other constraints. With a negative  $\varphi_{B_d}$ ,  $\sin 2\beta$  is larger than  $S_{\psi K_S}$ , implying a higher value on  $|\varepsilon_K|$ , in reasonable agreement with data and a better Unitary Triangle fit.

In both scenarios, new physics contributions to other observables, such as  $\Delta M_{B_{d,s}}$ , are expected and a dedicate analysis is necessary. In fact as we will see below the correlations between  $\varepsilon_K$  and  $\Delta M_{B_{d,s}}$  are powerful tests of the ability of MGF to describe properly all data on  $\Delta F = 2$  observables.

## 6.2 Input Parameters and the Parameter Space of the Model

Before proceeding with our numerical analysis, it is necessary to fix the input parameters and to define the parameter space of the model.

$G_F = 1.16637(1) \times 10^{-5} \text{ GeV}^{-2}$ [42]	$m_{B_d} = 5279.5(3) \text{ MeV}$ [42]
$M_W = 80.399(23) \text{ GeV}$ [42]	$m_{B_s} = 5366.3(6) \text{ MeV}$ [42]
$\sin^2 \theta_W = 0.23116(13)$ [42]	$F_{B_d} = 205(12) \text{ MeV}$ [35]
$\alpha(M_Z) = 1/127.9$ [42]	$F_{B_s} = 250(12) \text{ MeV}$ [35]
$\alpha_s(M_Z) = 0.1184(7)$ [42]	$\hat{B}_{B_d} = 1.26(11)$ [35]
$m_u(2 \text{ GeV}) = 1.7 \div 3.1 \text{ MeV}$ [42]	$\hat{B}_{B_s} = 1.33(6)$ [35]
$m_d(2 \text{ GeV}) = 4.1 \div 5.7 \text{ MeV}$ [42]	$F_{B_d} \sqrt{\hat{B}_{B_d}} = 233(14) \text{ MeV}$ [35]
$m_s(2 \text{ GeV}) = 100^{+30}_{-20} \text{ MeV}$ [42]	$F_{B_s} \sqrt{\hat{B}_{B_s}} = 288(15) \text{ MeV}$ [35]
$m_c(m_c) = (1.279 \pm 0.013) \text{ GeV}$ [43]	$\xi = 1.237(32)$ [35]
$m_b(m_b) = 4.19^{+0.18}_{-0.06} \text{ GeV}$ [42]	$\eta_B = 0.55(1)$ [44, 45]
$M_t = 172.9 \pm 0.6 \pm 0.9 \text{ GeV}$ [42]	$\tau_{B^\pm} = (1641 \pm 8) \times 10^{-3} \text{ ps}$ [42]
$m_K = 497.614(24) \text{ MeV}$ [42]	$ V_{us}  = 0.2252(9)$ [42]
$F_K = 156.0(11) \text{ MeV}$ [35]	$ V_{cb}  = (40.6 \pm 1.3) \times 10^{-3}$ [42]
$\hat{B}_K = 0.737(20)$ [35]	$ V_{ub}^{\text{incl.}}  = (4.27 \pm 0.38) \times 10^{-3}$ [42]
$\kappa_\epsilon = 0.94(2)$ [22]	$ V_{ub}^{\text{excl.}}  = (3.38 \pm 0.36) \times 10^{-3}$ [42]
$\varphi_\epsilon = (43.51 \pm 0.05)^\circ$ [22]	$\gamma = (73^{+22}_{-25})^\circ$ [42]
$\eta_1 = 1.87(76)$ [40]	
$\eta_2 = 0.5765(65)$ [44]	
$\eta_3 = 0.496(47)$ [39]	

Table 3: Values of experimental and theoretical quantities used throughout our numerical analysis. Notice that  $m_i(m_i)$  are the masses  $m_i$  at the scale  $m_i$  in the  $\overline{MS}$  scheme.  $M_t$  is the pole top-quark mass.

### 6.2.1 Input Parameters

In Table 3 we list the nominal values of the input parameters that we will use for the numerical analysis, except when otherwise stated. At this stage it is important to recall the theoretical and the experimental uncertainties on some relevant parameters and on the observables we shall study.

Considering the  $K^0 - \bar{K}^0$  mixing, remarkable improvements have been made in the case of the CP-violating parameter  $\varepsilon_K$ , where the decay constant  $F_K$  is known within 1% accuracy. Moreover the parameter  $\hat{B}_K$  is known within 3% accuracy from lattice calculations with dynamical fermions [33] and an improved estimate of *long distance* contributions to  $\varepsilon_K$  reduced this uncertainty down to 2% [22, 23]. The NNLO QCD corrections to  $\eta_1$  and  $\eta_3$  [39, 40] allowed to access the remaining scale uncertainties that amount according to [40] to roughly 6%, dominantly due to the uncertainty in  $\eta_1$ . Including also parametric uncertainties, dominated by the value of  $|V_{cb}|$ , Brod and Gorbahn estimate conservatively the present error in  $\varepsilon_K$  to amount to roughly 15% [40]. The reduction of this total error down to 7% in the coming years appears to be realistic. Further reduction will require progress both in the evaluation of long distance contributions and in  $\eta_1$ .  $\Delta M_K$  is very accurately measured, but is subject to poorly known long distance contributions.

Regarding the  $B_q^0 - \bar{B}_q^0$  mixings, lattice calculations considerably improved in recent

years reducing the uncertainties in  $F_{B_s}$ <sup>5</sup> and  $F_{B_d}$  and also in  $\sqrt{\hat{B}_{B_s}F_{B_s}}$  and  $\sqrt{\hat{B}_{B_d}F_{B_d}}$  down to 5%. This implies an uncertainty of 10% in  $\Delta M_{B_d}$  and  $\Delta M_{B_s}$  within the SM. On the other hand, the mixing induced CP-asymmetries  $S_{\psi\phi}$  and  $S_{\psi K_S}$  have much smaller hadronic uncertainties.

The hadronic uncertainties in the ratio  $R_{\Delta M_B}$  are roughly at the 3% level; the theoretical error on the  $b$  semileptonic CP-asymmetry  $A_{sl}^b$  is around the 20% level; the theoretical uncertainties in the rate of the  $\bar{B} \rightarrow X_s \gamma$  decay are below 10%; given the 5% uncertainty on  $F_{B_q}$  decay functions, the branching ratio for  $B^+ \rightarrow \tau^+ \nu$  has a theoretical error around the 10% and a large parametric error due to  $|V_{ub}|$ .

We stress that the situation with other  $B_i$  parameters, describing the hadronic matrix elements of  $\Delta F = 2$  operators absent in the SM, is much worse. Here a significant progress is desired.

On the experimental side,  $\varepsilon_K$ ,  $\Delta M_{B_d}$ ,  $\Delta M_{B_s}$  and the ratio  $R_{\Delta M_B}$  are very precisely measured with errors below the 1% level.  $S_{\psi K_S}$  is known with an uncertainty of  $\pm 3\%$  and the rate for the branching ratio of the  $\bar{B} \rightarrow X_s \gamma$  decay is known within 10%. On the contrary, larger experimental uncertainties affect the measurements of  $S_{\psi\phi}$  in D0 and LHCb, which differ from one another by an order of magnitude, but are still in agreement within the  $2\sigma$ -level, due to the large errors of the single determinations.  $A_{sl}^b$  has only been measured by D0 its experimental error is around the 20%. Similarly,  $BR(B^+ \rightarrow \tau^+ \nu)$  is plagued by the same uncertainty.

## 6.2.2 The CKM Matrix

To evaluate the observables we need to specify the values of the CKM elements. As already stated in sec. 2, the CKM matrix in this model is not unitary and is defined by

$$\tilde{V} = c_{uL} V c_{dL}, \quad (6.3)$$

where  $V$  is by construction a unitary  $3 \times 3$  matrix and  $c_{(u,d)L}$  are the cosines encoding the mixing between SM and exotic fermions. From eqs. (2.8) and (2.10), we deduce that  $c_{(u,d)L} \approx 1$ , except for  $t$  and  $t'$ . As a result, within an excellent accuracy the CKM matrix reads

$$\tilde{V} \simeq \begin{pmatrix} V_{ud} & V_{us} & V_{ub} \\ V_{cd} & V_{cs} & V_{cb} \\ c_{uL3} V_{td} & c_{uL3} V_{ts} & c_{uL3} V_{tb} \end{pmatrix}. \quad (6.4)$$

In this approximation, the deviation from the unitarity of the CKM matrix is

$$(\tilde{V}^\dagger \tilde{V})_{ij} = \delta_{ij} - s_{uL3}^2 V_{ti}^* V_{tj}, \quad (\tilde{V} \tilde{V}^\dagger)_{ij} = \delta_{ij} - s_{uL3}^2 \delta_{it} \delta_{jt}, \quad (6.5)$$

The deviations are present only when the top-quark entries are considered and are proportional to  $s_{uL3}^2$ . All other entries of the CKM matrix coincide with the corresponding entries of the unitary matrix  $V$  up to negligible corrections.

---

<sup>5</sup>Recently a remarkably precise value for  $F_{B_s}$  was reported in Ref. [46]:  $F_{B_s} = (225 \pm 4) \text{ MeV}$ . Still, we shall adopt a conservative approach and use the value of  $F_{B_s} = (250 \pm 12) \text{ MeV}$  in our analysis except when explicitly stated.

The important implication of the latter finding is that the angle  $\gamma$  in the unitary triangle is unaffected by such deviations. In the approximation of eq. (6.4),

$$\tilde{\gamma} \equiv \arg \left( -\frac{\tilde{V}_{ud} \tilde{V}_{ub}^*}{\tilde{V}_{cd} \tilde{V}_{cb}^*} \right) = \arg \left( -\frac{V_{ud} V_{ub}^*}{V_{cd} V_{cb}^*} \right), \quad (6.6)$$

and thus  $\gamma$  does not depend on  $c_{uL3}$  or  $s_{uL3}$ .

We state now how we fix the values of the CKM elements. From the tree-level experimental determinations of  $|V_{us}|$ ,  $|V_{cb}|$ ,  $|V_{ub}|$  and  $\gamma$ , we fix the corresponding parameters of  $\tilde{V}$ . In this way, also the corresponding parameters of the  $V$  matrix are univocally fixed and using the unitarity of  $V$ , we evaluate all the other entries of  $V$ . With all entries of  $V$  fixed we compute the masses and mixings of all fermions and flavour gauge bosons by means of eqs. (2.6)–(2.16). Finally, knowing  $c_{uL3}$ , we also determine the elements of the third row of  $\tilde{V}$ .

### 6.2.3 The Parameter Space of the Model

Having determined  $V$  what remains is the calculation of the spectrum and the couplings of NP particles. In principle they are fixed once, in addition to the SM parameters, we fix the *seven* NP couplings  $\lambda_{u,d}^{(\prime)}$ ,  $g_Q$ ,  $g_U$ ,  $g_D$  and the *two* mass parameters  $M_u$  and  $M_d$  in eqs. (2.2) and (2.3). Still, their actual determination is subtle since the energy scale at which the see-saw relations of eqs. (2.6) hold is a priori not known. We identify this scale with the mass of the lightest flavour gauge boson.

We fix the spectrum and the see-saw scale iteratively using the condition that all exotic masses are above  $m_t(m_t)$ . As a first step we evaluate the see-saw relation at  $m_t(m_t)$  to obtain a rough estimate of the masses of exotic fermions and lightest gauge boson. With this initial spectrum we run the masses of the SM fermions to the newly defined see-saw scale including all intermediate exotic fermion thresholds. The evaluation of the see-saw relation corrects the NP spectrum. We repeat the procedure until the values of exotic fermion masses and see-saw scale no longer change. Lastly, we evolve the exotic fermion masses down to the EW scale.

For the numerical analysis it is necessary to scan the parameter space of the model. We choose  $\lambda_{u,d} \in (0, 1.5]$  and all other couplings  $\{\lambda'_{u,d}, g_Q, g_U, g_D\} \in (0, 1.1]$  to stay in the perturbative regime of the theory. The two mass parameters are varied between  $M_u \in [100 \text{ GeV}, 1 \text{ TeV}]$  and  $M_d \in [30 \text{ GeV}, 250 \text{ GeV}]$  following the discussion in Ref. [12]. Unphysical points of the parameter space, namely cases with  $s_{u,d}$  or  $c_{u,d}$  larger than 1, are not considered. Larger  $M_u$  and  $M_d$  values decouple the NP from the SM and are therefore phenomenologically irrelevant. With respect to the analysis of Ref. [12] we are scanning over all NP parameters, including  $\lambda'_{u,d}$  and  $g_Q, g_U, g_D$ .

## 6.3 Results

To present the features of the MGF model we are discussing, we use  $|V_{us}|$  and  $|V_{cb}|$  at their central values in tab. 3 and

$$|V_{ub}| = 3.38 \times 10^{-3} \quad \text{and} \quad \gamma = 68^\circ, \quad (6.7)$$

which are among the favoured values within the SM when the experimental values of both  $S_{\psi K_S}$  and  $R_{\Delta M_B}$  are taken into account.

With this CKM matrix we list in tab. 4 the central values for the SM predictions of the observables under consideration together with their experimental determinations.

SM predictions for exclusive $ V_{ub} $	Experimental values
$\Delta M_{B_d} = 0.592 \text{ ps}^{-1}$	$\Delta M_{B_d} = 0.507(4) \text{ ps}^{-1}$ [42]
$\Delta M_{B_s} = 20.28 \text{ ps}^{-1}$	$\Delta M_{B_s} = 17.77(12) \text{ ps}^{-1}$ [42]
$R_{\Delta M_B} = 2.92 \times 10^{-2}$	$R_{\Delta M_B} = (2.85 \pm 0.03) \times 10^{-2}$ [42]
$S_{\psi K_S} = 0.671$	$S_{\psi K_S} = 0.673(23)$ [42]
$S_{\psi\phi} = 0.0354$	$\phi_s^{\psi\phi} = 0.55^{+0.38}_{-0.36}$ [47, 48]
	$\phi_s^{\psi\phi} = 0.03 \pm 0.16 \pm 0.07$ [49]
$\Delta M_K = 0.4627 \times 10^{-2} \text{ ps}^{-1}$	$\Delta M_K = 0.5292(9) \times 10^{-2} \text{ ps}^{-1}$ [42]
$ \epsilon_K  = 1.791 \times 10^{-3}$	$ \epsilon_K  = 2.228(11) \times 10^{-3}$ [42]
$A_{sl}^b = -0.0233 \times 10^{-2}$	$A_{sl}^b = (-0.787 \pm 0.172 \pm 0.093) \times 10^{-2}$ [27]
$BR(b \rightarrow s\gamma) = 3.15 \times 10^{-4}$	$BR(b \rightarrow s\gamma) = (3.55 \pm 0.24 \pm 0.09) \times 10^{-4}$ [42]
$BR(B^+ \rightarrow \tau^+\nu) = 0.849 \times 10^{-4}$	$BR(B^+ \rightarrow \tau^+\nu) = (1.65 \pm 0.34) \times 10^{-4}$ [42]
$R_{BR/\Delta M} = 1.43 \times 10^{-4} \text{ ps}$	$R_{BR/\Delta M} = (3.25 \pm 0.67) \times 10^{-4} \text{ ps}$

Table 4: The SM predictions for the observables we shall consider using the exclusive determination of  $|V_{ub}|$  and the corresponding experimental values.

Comparing these results with the data we make the following observations

- $|\epsilon_K|$  is smaller than its experimental determination, while  $S_{\psi K_S}$  is very close to the central experimental value, as it should be for the chosen  $|V_{ub}|$  and  $\gamma$ .
- The mass differences  $\Delta M_{B_d}$  and  $\Delta M_{B_s}$  are visibly above the data; also their ratio  $R_{\Delta M_B}$  is above the experimental determination, but in agreement at the  $3\sigma$  level.
- $BR(B^+ \rightarrow \tau^+\nu)$  is well below the data and consequently also the ratio  $R_{BR/\Delta M}$  turns out to be below the measured central value by more than a factor of two. Even if the experimental error in  $BR(B^+ \rightarrow \tau^+\nu)$  is large, the parameter space of the model is strongly constrained. Furthermore, from the correlation among  $R_{\Delta M_B}$  and  $R_{BR/\Delta M}$  it is evident that the model can only deteriorate the SM tension in these observables.
- Concerning  $S_{\psi\phi}$ , the predicted value is consistent with the most recent data from CDF, D0 and LHCb.
- $A_{sl}^b$  is well below the D0 data.
- Finally the predicted central value for  $BR(\bar{B} \rightarrow X_s\gamma)$  is smaller than the central experimental value but consistent with it within the  $2\sigma$  error range.

Any NP model that aims to remove or soften the anomalies listed above should simultaneously:

1. Enhance  $|\epsilon_K|$  by roughly 20% without affecting significantly  $S_{\psi K_S}$ .



2. Suppress  $\Delta M_{B_d}$  and  $\Delta M_{B_s}$  by roughly 15% and 10%, respectively.
3. Slightly suppress  $R_{\Delta M_B}$  by 3%.
4. Strongly enhance  $R_{BR/\Delta M}$  by 130%.
5. Moderately enhance the value  $BR(\bar{B} \rightarrow X_s \gamma)$  by 5 – 10%.

As we shall see below, the model naturally satisfies requirements 1., 3. and 5. On the other side, it fails in 2. and 4.: indeed the mass differences  $\Delta M_{B_{d,s}}$  can only be enhanced with respect to the corresponding would-be SM value; this enhancement is predicted to be significant if one requires to solve the  $|\varepsilon_K|$ - $S_{\psi K_S}$  anomaly. Furthermore, the predicted value for the  $R_{BR/\Delta M}$  can only be decreased, resulting in a tension on this observable more serious than in the SM.

In what follows we will look closer at the pattern of flavour violations in the MGF still keeping the input parameters at their central values. Subsequently we will comment on how some of our statements are softened when hadronic uncertainties in the input parameters are taken into account.

Considering now the NP contributions within MGF, we find the following pattern of effects:

- If we neglect the contributions of flavour gauge bosons and of exotic quarks, i.e. considering only the would-be SM contributions, the mixing amplitudes  $M_{12}^i$  and  $BR(\bar{B} \rightarrow X_s \gamma)$  are reduced with respect to the SM ones due to the modification of the CKM matrix, encoded in the mixings  $c_{u,d_L}$ . As a result, once the third-row entries of the CKM matrix are involved, the would-be SM values of the considered observables are smaller than the values reported in tab. 4.
- The RR flavour gauge boson contributions are negligible for all observables in all the parameter space. We shall not consider such contributions in the following description.
- $|\varepsilon_K|$  is uniquely enhanced by the new box-diagram contributions involving exotic quarks, while it is uniquely suppressed by heavy gauge flavour boson contributions. Among the latter, the  $LR$  contributions are the dominant ones, while the  $LL$  ones are safely negligible.
- $\Delta M_{B_{d,s}}$  are also uniquely enhanced by the new box-diagram contributions, but are mostly unaffected by heavy flavour gauge boson contributions. This is in particular true for  $\Delta M_{B_d}$ , while for  $\Delta M_{B_s}$  the latter contributions can be non-negligible either enhancing or suppressing it. This is best appreciated when considering the ratio  $R_{\Delta M_B}$ : this observable does not show any dependence on the new box-diagram contributions, since in MGF the operator structure in box-diagram contributions does not change with respect to the SM and the NP effects are the same in the  $B_d$  and  $B_s$  systems. As a result any NP effect in this ratio should be attributed to the heavy gauge flavour boson contributions, both  $LL$  and  $LR$ .

- The mixing induced CP-asymmetries  $S_{\psi K_S}$  and  $S_{\psi\phi}$  are unaffected by the new box-diagram contributions. Similarly to  $R_{\Delta M_B}$ , this allows to see transparently the heavy gauge flavour boson contributions, which was much harder in the case of  $\Delta M_{B_{d,s}}$ . We find that  $S_{\psi K_S}$  is only affected by  $LL$  contributions and can only be suppressed.  $S_{\psi\phi}$  depends on both  $LL$  and  $LR$  contributions. Interestingly, the NP contributions interfere destructively with the SM contribution such that the sign of  $S_{\psi\phi}$  can in principle be reversed in this model. Similar conclusions hold for  $A_{sl}^b$ : it is not affected by box-diagram contributions, the  $LR$  contributions are almost completely negligible and the  $LL$  ones are the only relevant enhancing  $|A_{sl}^b|$  towards the central value of the experimental determination.
- Finally, the branching ratio of  $\bar{B} \rightarrow X_s \gamma$  can be significantly affected by the modifications in the SM magnetic penguin contributions that can only enhance this observable, as already pointed out in Ref. [12]. The heavy gauge flavour boson contributions are negligible as discussed in Ref. [17].

Having listed the basic characteristic of NP contributions in this model we will now present our numerical results in more detail stressing the important role of correlations among various observables identified in this model by us for the first time.

### 6.3.1 Correlations Among the Observables

In this section we discuss correlations among the observables. They will allow us to constrain the parameter space of the model and see whether this model is able or not to soften, or even solve, the anomalies in the flavour data.

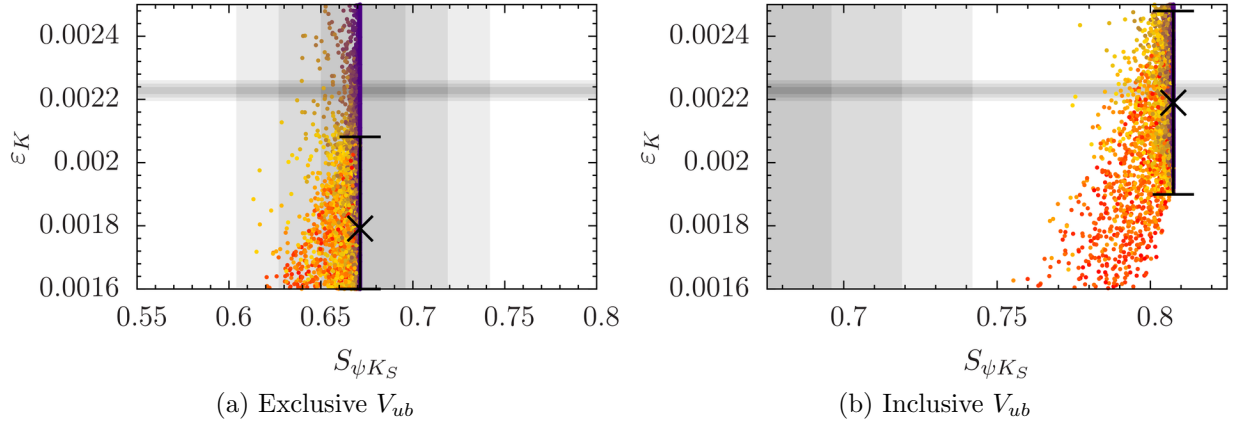


Figure 3: The correlation of  $\varepsilon_K$  and  $S_{\psi K_S}$ . The shaded grey regions are the experimental  $1\sigma$ - $3\sigma$  error ranges, while the cross is the central SM values reported in tab. 4. The colour of the points represent the percentage of the box-diagram contributions (purple) and of the flavour gauge boson ones (red) in  $\varepsilon_K$ . In the NP points the theoretical error on  $\varepsilon_K$  is included.

In fig. 3a, we show the correlation between  $\varepsilon_K$  and  $S_{\psi K_S}$ . The plot confirms that the exclusive value of  $|V_{ub}|$  is favoured in this model. Indeed the NP contributions are able to solve the  $\varepsilon_K$ - $S_{\psi K_S}$  anomaly in a reasonably large region of the parameters space. This happens when the  $\varepsilon_K$  prediction approaches the data due to box-diagram contributions (purple points), while  $S_{\psi K_S}$  is mostly unaffected. This is in particular possible when the flavour gauge bosons contributions are negligible. When the flavour gauge boson contributions are significant (red points)  $S_{\psi K_S}$  is uniquely suppressed relatively to the SM value. However, as seen in the figure a combination of large box contributions as well as flavour gauge boson contributions (yellow points) allows bringing  $\varepsilon_K$  in agreement with the data while keeping  $S_{\psi K_S}$  within the  $2\sigma$  experimental error range.

On the other hand, points for which the box contributions are negligible and instead the flavour gauge boson contributions dominate in  $\varepsilon_K$  (purely red points) cannot explain the observed value of  $\varepsilon_K$ . However, this kind of contributions are best suited for the case with the inclusive determination of  $|V_{ub}|$ , reported in fig. 3b. Still, there exist no points, which simultaneously bring  $\varepsilon_K$  and  $S_{\psi K_S}$  in a  $3\sigma$  agreement. The flavour gauge bosons contributions are not large enough to suitably correct  $S_{\psi K_S}$ . We conclude that the inclusive determination of  $|V_{ub}|$  is disfavoured in this model and we shall not further pursue this case.

In fig. 4, we present the correlations between  $\varepsilon_K$  and  $\Delta M_{B_{d,s}}$ . From (a) and (b), we conclude that the model cannot solve the  $|\varepsilon_K| - S_{\psi K_S}$  anomaly present in the SM, without worsening the already moderate agreement of this model with the  $\Delta M_{B_{d,s}}$  experimental data. Indeed the values  $\Delta M_{B_d} \approx 0.75/ps$  and  $\Delta M_{B_s} \approx 27/ps$  are so larger that in the case that the central values of the weak decay constants  $F_{B_{d,s}}$  do not change in the future, but their and other input parameter uncertainties are further reduced, we will have to conclude that the model fails to describe the  $\Delta F = 2$  data.

However, we should emphasise that this problem could be avoided if the values for the weak decay constants  $F_{B_{d,s}}$  are smaller than the ones used in the plots (a) and (b). Indeed, in (c) we adopt a 15% reduced value for  $F_{B_d}$ , close to its  $3\sigma$  value, while in (d) the last determination of  $F_{B_s}$  reported in Ref. [46]. This input, modifies the SM values to be

$$\Delta M_{B_d} = 0.43 \text{ ps}^{-1} \quad \text{and} \quad \Delta M_{B_s} = 16.4 \text{ ps}^{-1}, \quad (6.8)$$

such that now the enhancements of these observables by NP is welcomed by the data. From plots (c) and (d) we deduce that the NP contributions and the requirement of agreement of  $|\varepsilon_K|$  with data within MGF automatically enhance  $\Delta M_{B_{d,s}}$ . Even if also in this case  $\Delta M_{B_{d,s}}$  are found above the data, the model is performing much better than in the previous case. This exercise shows that on one hand it is crucial to get a better control over hadronic parameters in order to obtain a clearer picture of NP contributions and on the other hand that other more precise observables should be analysed until the uncertainties on  $\Delta M_{B_{d,s}}$  are lowered.

In fig. 5, we show the correlation between the ratio of the mass differences,  $R_{\Delta M_B}$ , and the ratio among the branching ratio of the  $B^+ \rightarrow \tau^+ \nu$  decay and the  $\Delta M_{B_d}$ ,  $R_{BR/\Delta M}$ . Both observables have negligible theoretical uncertainties and are therefore very useful to provide strong constraints on the parameter space. On the left, the red points correspond to an  $\varepsilon_K$  prediction in agreement with the data at  $3\sigma$ , while the blue ones do not satisfy the  $\varepsilon_K$  constraint. This plot largely constrains the parameter space of the model; for only very few points  $\varepsilon_K$ ,  $R_{\Delta M_B}$  and  $R_{BR/\Delta M}$  agree at  $3\sigma$ -level with the data simultaneously.

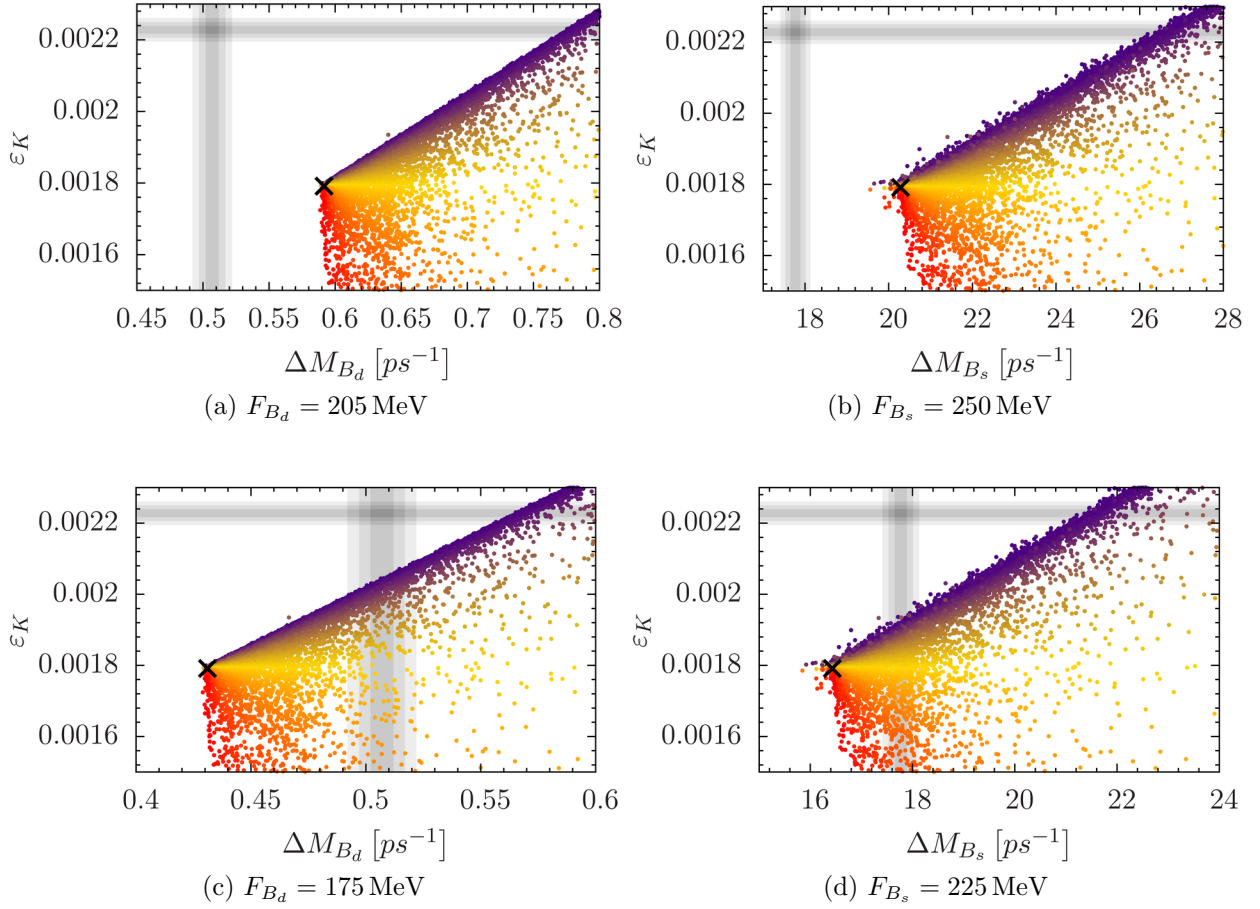


Figure 4: Correlation plot of  $\varepsilon_K$  with  $\Delta M_{B_d}$  and  $\Delta M_{B_s}$  on the left and right, respectively. In the upper plots, we use for  $F_{B_{d,s}}$  the values reported in tab. 3, while for the lower plots we adopt smaller values:  $F_{B_d}$  is reduced down to 85% of its value, close to the  $3\sigma$  error level and  $F_{B_s}$  is taken to be the new determination reported in Ref. [46]. In the plots above we have not included the  $1\sigma$  error in  $\varepsilon_K$  to best illustrate the interplay of box- (purple) and tree-contributions (red).

Furthermore, all red points correspond to values for  $R_{BR/\Delta M}$  smaller than the SM prediction and therefore the model can only worsen the SM tension. In the case that the experimental sensitivity to the  $BR(B^+ \rightarrow \tau^+ \nu)$  improves, it will be possible to further constrain and possibly exclude the present MGF model.

Having reduced the parameter space, we concentrate now on a few other predictions of the model. In fig. 6, we show the  $m_{t'} - \hat{M}_{A^{24}}$  parameter space, where  $m_{t'}$  is the mass of the exotic partner of the top-quark and  $\hat{M}_{A^{24}}$  the mass of the lightest neutral gauge boson; the corresponding particles have the best chances to be detected at the LHC. The red and blue points are those identified in fig. 5 to agree and disagree in  $R_{\Delta M_B}$ ,  $R_{BR/\Delta M}$  and  $\varepsilon_K$  with the data at the  $1\sigma$ - $3\sigma$  level, respectively.

Interestingly, the phenomenological results presented above hold not only for light but

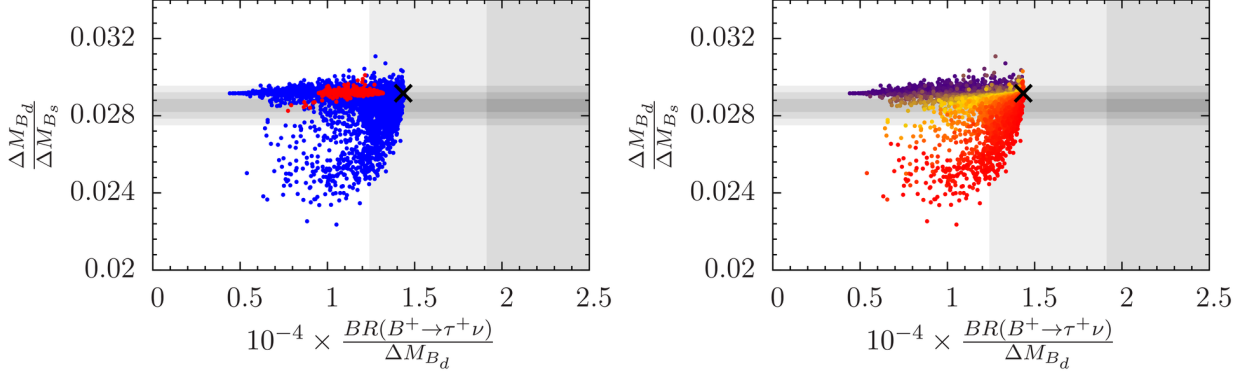


Figure 5: Correlation plot for  $R_{\Delta M_B}$  and  $R_{BR/\Delta M}$ . The grey regions refer to the experimental  $1\sigma$ - $3\sigma$  and  $2\sigma$ - $3\sigma$  error ranges for  $R_{\Delta M_B}$  and  $R_{BR/\Delta M}$ , respectively. The big black point refers to the SM values reported in tab. 4. On the left, red (blue) points refer to agreement (disagreement) of the points prediction of  $\varepsilon_K$  and the data at  $3\sigma$  level. On the right the colours represent contribution of boxes and trees in  $\varepsilon_K$ .

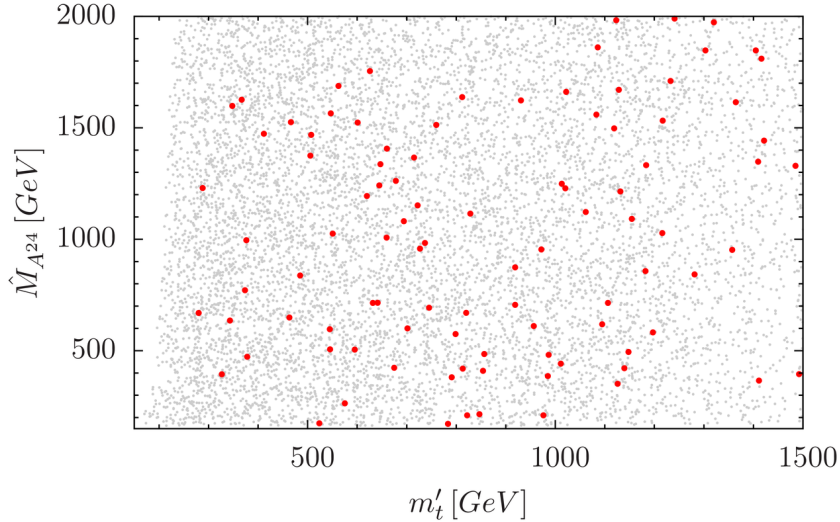


Figure 6:  $m_{t'} - \hat{M}_{A^{24}}$  parameter space. For all red points in the plot  $R_{\Delta M_B}$ ,  $R_{BR/\Delta M}$  and  $\varepsilon_K$  agree with the data at  $3\sigma$ -level.

also for heavy  $t'$ 's. Also the mass of the lightest flavour gauge boson is not bounded.

Furthermore, in fig. 7 we show two correlation plots which represent also clear predictions for this model. Plot (a) is the correlation for  $S_{\psi\phi}$  and  $A_{sl}^b$  showing that only tiny deviations from the SM values are allowed: this turns out to be an interesting result for  $S_{\psi\phi}$ , which is indeed close to the recent determination of LHCb. On the other hand,  $A_{sl}^b$  has only been measured by D0, but hopefully LHCb will also have something to say in the near future. Once the experimental uncertainties are lowered, such clear predictions will be essential to provide the final answer on how well this model performs.

In plot (b), we show the correlation of  $BR(\bar{B} \rightarrow X_s \gamma)$  and  $m_{t'}$ . We confirm the finding

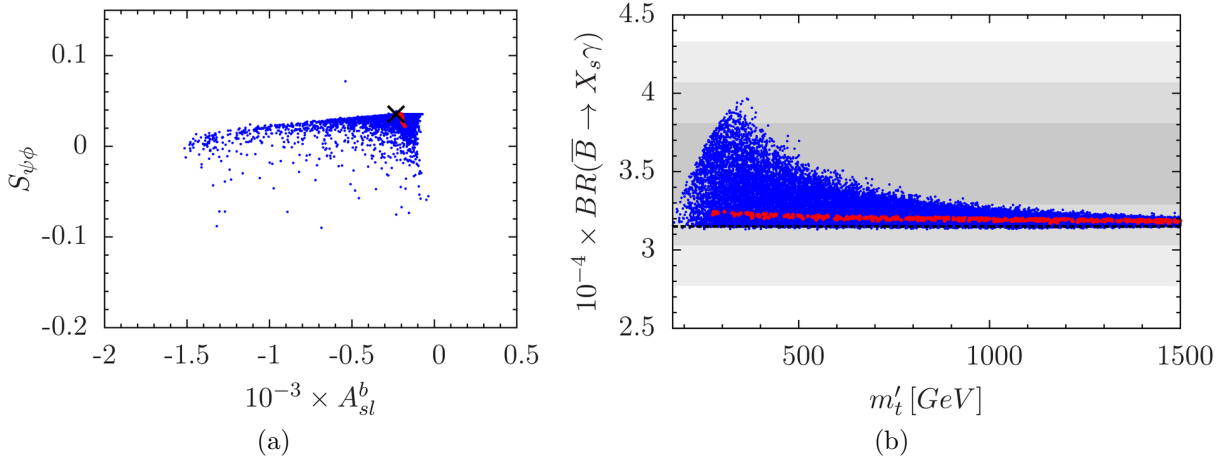


Figure 7: Correlation plot of  $S_{\psi\phi}$  and  $A_{sl}^b$  on the left and  $BR(\bar{B} \rightarrow X_s \gamma)$  and  $m'_t$  on the right. Grey regions refer to the experimental error ranges. The big black point refers to the SM values reported in tab. 4. In red the points for which  $R_{\Delta MB}$ ,  $R_{BR/\Delta M}$  and  $\varepsilon_K$  agree with the data at  $3\sigma$  level, in blue all others for which there is no agreement.

of Grinstein *et al.* that in this model the NP contributions to  $BR(B \rightarrow X_s \gamma)$  always enhance it towards the central experiment value. However, interestingly only very small enhancements of this branching ratio are allowed when also the bounds from  $\Delta F = 2$  observables are taken into account.

## 7 Comparison with other Models

A complete comparison of the patterns of flavour violation in MGF with corresponding patterns found in numerous models [50] would require the study of  $\Delta F = 1$  processes, however already  $\Delta F = 2$  observables allow a clear distinction between the MGF and the simplest extensions of the SM. Here we just quote a few examples:

- In the original MFV framework restricted to LL operators, the so-called constrained MFV [51], the  $|\varepsilon_K| - S_{\psi K_S}$  anomaly can only be solved by enhancing  $|\varepsilon_K|$  since in this framework  $S_{\psi K_S}$  remains SM-like. In this framework then only the exclusive value of  $|V_{ub}|$  is viable. An example of such a framework is the model with a single universal extra dimension (UED) for which a very detailed analysis of  $\Delta F = 2$  observables has been performed in [52]. In fact this is a general property of CMFV models as demonstrated in [53]. Thus after  $|\varepsilon_K|$  has been taken into account and contributions from tree-level heavy gauge boson exchanges have been eliminated MGF resembles CMFV if only  $\Delta F = 2$  processes are considered. However  $\Delta F = 1$  processes can provide a distinction. In fact whereas in MGF the NP contributions uniquely enhance  $BR(\bar{B} \rightarrow X_s \gamma)$ , in UED they uniquely suppress this branching ratio [54]. Concerning the  $|\varepsilon_K| - \Delta M_{B_{d,s}}$  tension MGF and CMFV are again similar.



- The 2HDM framework with MFV and flavour blind phases, the so-called  $2\text{HDM}_{\overline{\text{MFV}}}$  [55], can on the other hand be easily distinguished from MGF. In this model NP contributions to  $\varepsilon_K$  are tiny and the inclusive value of  $|V_{ub}|$  is required in order to obtain the correct value of  $|\varepsilon_K|$ . The interplay of the CKM phase with the flavour blind phases in Yukawa couplings and Higgs potential suppress  $S_{\psi K_S}$  simultaneously enhancing the asymmetry  $S_{\psi\phi}$ . As in the case of MGF this asymmetry is SM-like or has a reversed sign. It is  $S_{\psi\phi}$  together with the value of  $|V_{ub}|$  which will distinguish MGF from  $2\text{HDM}_{\overline{\text{MFV}}}$ .
- Finally, let us mention the left-right asymmetric model (LRAM) for which a very detailed FCNC analysis has been recently presented in [56]. As this model has many free parameters both values of  $|V_{ub}|$ , inclusive and exclusive, are valid. The model contains many new phases and the  $|\varepsilon_K| - S_{\psi K_S}$  anomaly can be solved in many ways. Moreover, the model struggles with the  $\varepsilon_K$  constraint due to huge neutral Higgs tree-level contributions. However, as demonstrated in Section 7 of that paper a simple structure of the right-handed mixing matrix gives a transparent solution to the  $|\varepsilon_K| - S_{\psi K_S}$  anomaly by enhancing  $|\varepsilon_K|$ , keeping  $S_{\psi K_S}$  at the SM value and in contrast to MGF automatically *suppressing*  $\Delta M_{B_{d,s}}$  and significantly *enhancing*  $S_{\psi\phi}$ . While MGF falls back in this comparison, one should emphasise that on the MGF has very few parameters and provides the explanation of quark masses and mixings, while this is not the case in the LRAM.

## 8 Conclusion

We have presented an extensive analysis of  $\Delta F = 2$  observables and  $B \rightarrow X_s \gamma$  for a specific MGF model presented in Ref. [12]. In particular we included tree-level contributions due to the presence of heavy flavour gauge bosons, that have been considered in our analysis for the first time.

Our main findings are as follows. The model predicts a clear pattern of deviations from the SM:

- Enhancements of  $|\varepsilon_K|$  and  $\Delta M_{B_{d,s}}$  in a correlated manner by new box-diagram contributions and suppression of  $|\varepsilon_K|$  by tree-level heavy gauge boson contributions with only small impact on  $\Delta M_{B_{d,s}}$ .
- Mixing induced CP-asymmetries  $S_{\psi K_S}$  and  $S_{\psi\phi}$  are unaffected by box-diagram contributions, but receive sizeable destructive contributions from tree-level heavy gauge boson exchanges such that the sign of  $S_{\psi\phi}$  can be reversed. However, these effects are basically eliminated once the  $\varepsilon_K$  constraint is taken into account.
- The  $\varepsilon_K - S_{\psi K_S}$  anomaly present in the SM is removed through the enhancement of  $|\varepsilon_K|$ , leaving  $S_{\psi K_S}$  practically unmodified. This is achieved with the help of box-diagram contributions in the regions of the parameter space for which they are dominant over heavy flavour gauge boson contributions, which interfere destructively with the SM amplitudes.



- This structure automatically implies that in this model the exclusive determination of  $|V_{ub}|$  is favoured.
- $b$  semileptonic CP-asymmetry  $A_{sl}^b$ , that a priori could receive large contributions from the tree-level flavour gauge boson diagrams, remains close to the SM values once requiring  $|\varepsilon_K|$  to be in agreement with the data.
- Most importantly, the  $\varepsilon_K$  constraint implies the central values of  $\Delta M_{B_{d,s}}$  to be roughly 50% higher than the very precise data. This disagreement cannot be cured fully by hadronic uncertainties although significant reduction in the values of  $F_{B_{d,s}}$  could soften this problem.
- We have pointed out that the ratio of the mass differences,  $\Delta M_{B_d}/\Delta M_{B_s}$  and the ratio of the  $B^+ \rightarrow \tau^+ \nu$  branching ratio and  $\Delta M_{B_d}$ , together with  $\varepsilon_K$ , provide strong constraints on the parameter space of the model. Furthermore, the correlation among these two observables encodes a serious tension on the flavour data that can only be deteriorated in the model.
- In agreement with Ref. [12], we find that  $BR(B \rightarrow X_s \gamma)$  is naturally enhanced in this model, bringing the theory closer to the data, still only small corrections are allowed by the  $\Delta F = 2$  bounds.
- We have demonstrated how this model can be distinguished by means of the flavour data from other extensions of the SM.

In summary, the great virtue of this model is its predictivity, such that within the coming years it will be evident whether it can be considered as a valid description of low-energy data. Possibly the most transparent viability tests of the model are the future values of  $F_{B_{d,s}}$  and  $|V_{ub}|$ . For the model to accommodate the data,  $F_{B_{d,s}}$  have to be reduced by 15% and  $|V_{ub}|$  has to be close to  $3.4 \times 10^{-3}$ . Violation of any of these requirements will put this extension of the SM in trouble. We emphasise that the triple correlation between  $\Delta M_{B_{d,s}}$ ,  $\varepsilon_K$  and  $S_{\psi K_S}$  was instrumental in reaching this conclusion. The same result is derived by the complementary study on the  $R_{BR/\Delta M} - R_{\Delta M_B}$  correlation. Our work shows that the study of correlations among flavour observables and the accuracy of non-perturbative parameters like  $\hat{B}_K$  and  $F_{B_{d,s}}$  are crucial for the indirect searches for physics beyond the Standard Model.

## Acknowledgements

We would like to thank Benjamín Grinstein for useful details on the Ref. [12] and Paride Paradisi for very interesting discussions. This research was done in the context of the ERC Advanced Grant project "FLAVOUR" (267104). The work of MVC has been partially supported by the Graduiertenkolleg GRK 1054 of DFG.

# A Feynman Rules for MGF

## A.1 Couplings of SM Gauge and Goldstone bosons

### $\gamma$ coupling

The photon coupling remains unchanged; proportional to the quark charges  $Q_u$  and  $Q_d$ .

### $G$ coupling

The gluon coupling remains unchanged; proportional to the colour generators  $\lambda_{SU(3)}^a$ .

### $W^\pm$ coupling

$$W^\pm \sim \text{wavy line} \rightarrow \begin{array}{l} \nearrow \bar{f} \\ \searrow f \end{array} = i \frac{e}{\sqrt{2} s_w} \gamma_\mu P_L C_L$$

with the actual values for  $\bar{f}$ ,  $f$  and  $C_L$ :

$$\begin{aligned} W^+ \bar{u}_i d_j &: C_L = c_{uLi} V_{ij} c_{dLj} \\ W^+ \bar{u}'_i d'_j &: C_L = s_{uLi} V_{ij} s_{dLj} \\ W^+ \bar{u}_i d'_j &: C_L = c_{uLi} V_{ij} s_{dLj} \\ W^+ \bar{u}'_i d_j &: C_L = s_{uLi} V_{ij} c_{dLj} \end{aligned}$$

$$\begin{aligned} W^- \bar{d}_j u_i &: C_L = c_{uLi} V_{ij}^* c_{dLj} \\ W^- \bar{d}'_j u'_i &: C_L = s_{uLi} V_{ij}^* s_{dLj} \\ W^- \bar{d}_j u'_i &: C_L = s_{uLi} V_{ij}^* c_{dLj} \\ W^- \bar{d}'_j u_i &: C_L = c_{uLi} V_{ij}^* s_{dLj} \end{aligned}$$

### $Z$ coupling

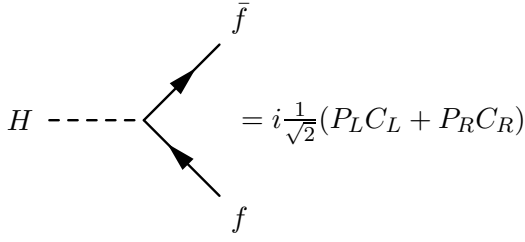
$$Z \sim \text{wavy line} \rightarrow \begin{array}{l} \nearrow \bar{f} \\ \searrow f \end{array} = i \frac{e}{s_w} \gamma_\mu (P_L C_L + P_R C_R)$$

with the actual values for  $\bar{f}$ ,  $f$  and  $C$ :

$$\begin{aligned} Z \bar{u}_i u_i &: C_R = -\frac{s_w^2}{c_w} Q_u \\ &: C_L = \frac{T_u^3 c_{uLi}^2 - s_w^2 Q_u}{c_w} \\ Z \bar{u}'_i u'_i &: C_R = -\frac{s_w^2}{c_w} Q_u \\ &: C_L = +\frac{T_u^3 s_{uLi}^2 - s_w^2 Q_u}{c_w} \\ Z \bar{u}_i u'_i &: C_R = 0 \\ &: C_L = +\frac{T_u^3}{c_w} c_{uLi} s_{uLi} \\ Z \bar{u}'_i u_i &: C_R = 0 \\ &: C_L = +\frac{T_u^3}{c_w} c_{uLi} s_{uLi} \end{aligned}$$

$$\begin{aligned} Z \bar{d}_i d_i &: C_R = -\frac{s_w^2}{c_w} Q_d \\ &: C_L = \frac{T_d^3 c_{dLi}^2 - s_w^2 Q_d}{c_w} \\ Z \bar{d}'_i d'_i &: C_R = -\frac{s_w^2}{c_w} Q_d \\ &: C_L = +\frac{T_d^3 s_{dLi}^2 - s_w^2 Q_d}{c_w} \\ Z \bar{d}_i d'_i &: C_R = 0 \\ &: C_L = +\frac{T_d^3}{c_w} c_{dLi} s_{dLi} \\ Z \bar{d}'_i d_i &: C_R = 0 \\ &: C_L = +\frac{T_d^3}{c_w} c_{dLi} s_{dLi} \end{aligned}$$

## H coupling

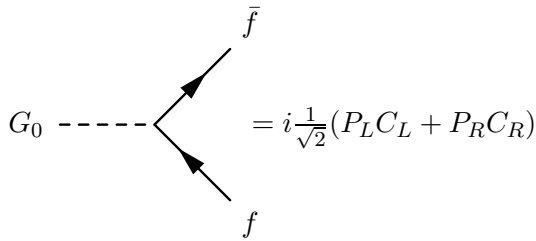


with the actual values for  $\bar{f}$ ,  $f$  and  $C$ :

$$\begin{aligned} H \bar{u}_i u_i & : C_R = C_L = +\lambda_u s_{uRi} c_{uLi} \\ H \bar{u}'_i u'_i & : C_R = C_L = -\lambda_u c_{uRi} s_{uLi} \\ H \bar{u}_i u'_i & : C_R = C_L = -\lambda_u c_{uRi} c_{uLi} \\ H \bar{u}'_i u_i & : C_R = C_L = +\lambda_u s_{uRi} s_{uLi} \end{aligned}$$

$$\begin{aligned} H \bar{d}_i d_i & : C_R = C_L = +\lambda_d s_{dRi} c_{dLi} \\ H \bar{d}'_i d'_i & : C_R = C_L = -\lambda_d c_{dRi} s_{dLi} \\ H \bar{d}_i d'_i & : C_R = C_L = -\lambda_d c_{dRi} c_{dLi} \\ H \bar{d}'_i d_i & : C_R = C_L = +\lambda_d s_{dRi} s_{dLi} \end{aligned}$$

## G<sub>0</sub> coupling

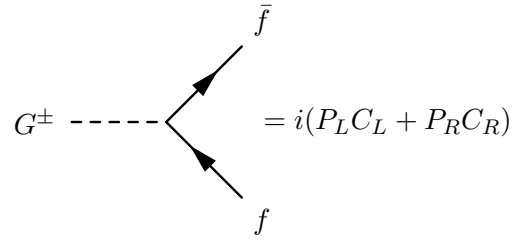


with the actual values for  $\bar{f}$ ,  $f$  and  $C$ :

$$\begin{aligned} G_0 \bar{u}_i u_i & : C_R = -C_L = -i \lambda_u s_{uRi} c_{uLi} \\ G_0 \bar{u}'_i u'_i & : C_R = -C_L = +i \lambda_u c_{uRi} s_{uLi} \\ G_0 \bar{u}_i u'_i & : C_R = -C_L = +i \lambda_u c_{uRi} c_{uLi} \\ G_0 \bar{u}'_i u_i & : C_R = -C_L = -i \lambda_u s_{uRi} s_{uLi} \end{aligned}$$

$$\begin{aligned} G_0 \bar{d}_i d_i & : C_R = -C_L = +i \lambda_d s_{dRi} c_{dLi} \\ G_0 \bar{d}'_i d'_i & : C_R = -C_L = -i \lambda_d c_{dRi} s_{dLi} \\ G_0 \bar{d}_i d'_i & : C_R = -C_L = -i \lambda_d c_{dRi} c_{dLi} \\ G_0 \bar{d}'_i d_i & : C_R = -C_L = +i \lambda_d s_{dRi} s_{dLi} \end{aligned}$$

## G<sup>±</sup> coupling



with the actual values for  $\bar{f}$ ,  $f$  and  $C_L$ :

$$\begin{aligned} G^+ \bar{u}_i d_j & : C_R = +\lambda_d c_{uLi} V_{ij} s_{dRj} \\ & : C_L = -\lambda_u s_{uRi} V_{ij} c_{dLj} \\ G^+ \bar{u}'_i d'_j & : C_R = -\lambda_d s_{uLi} V_{ij} c_{dRj} \\ & : C_L = +\lambda_u c_{uRi} V_{ij} s_{dLj} \\ G^+ \bar{u}_i d'_j & : C_R = -\lambda_d c_{uLi} V_{ij} c_{dRj} \\ & : C_L = +\lambda_u c_{uRi} V_{ij} c_{dLj} \\ G^+ \bar{u}'_i d_j & : C_R = +\lambda_d s_{uLi} V_{ij} s_{dRj} \\ & : C_L = -\lambda_u s_{uRi} V_{ij} s_{dLj} \end{aligned}$$

$$\begin{aligned} G^- \bar{d}_j u_i & : C_R = -\lambda_u s_{uRi} V_{ij}^* c_{dLj} \\ & : C_L = +\lambda_d c_{uLi} V_{ij}^* s_{dRj} \\ G^- \bar{d}'_j u'_i & : C_R = +\lambda_u c_{uRi} V_{ij}^* s_{dLj} \\ & : C_L = -\lambda_d s_{uLi} V_{ij}^* c_{dRj} \\ G^- \bar{d}_j u'_i & : C_R = +\lambda_u c_{uRi} V_{ij}^* c_{dLj} \\ & : C_L = -\lambda_d c_{uLi} V_{ij}^* c_{dRj} \\ G^- \bar{d}'_j u_i & : C_R = -\lambda_u s_{uRi} V_{ij}^* s_{dLj} \\ & : C_L = +\lambda_d s_{uLi} V_{ij}^* s_{dRj} \end{aligned}$$

## A.2 Couplings of Flavour Gauge Bosons

There are three types of flavour gauge bosons,  $A_Q^a$ ,  $A_U^a$ , and  $A_D^a$ , which are flavour eigenstates but not mass eigenstates. We denote the mass eigenstates with  $\hat{A}^m$ , where

$m = 1, \dots, 24$ .

$$\begin{aligned}\chi &= (A_Q^1, \dots, A_Q^8, A_U^1, \dots, A_U^8, A_D^1, \dots, A_D^8)^T \\ \varphi &= (\hat{A}^1, \dots, \hat{A}^{24})^T.\end{aligned}$$

Flavour basis  $\chi$  and mass basis  $\varphi$  are connected through the transformation

$$\chi = \mathcal{W}\varphi, \quad (\text{A.1})$$

where  $\mathcal{W}$  is obtained numerically by diagonalising the mass matrix in eq. (2.15) such that:

$$\hat{\mathcal{M}}_A^2 = \mathcal{W}^T \mathcal{M}_A^2 \mathcal{W} \quad (\text{A.2})$$

and  $\hat{\mathcal{M}}_A$  is a diagonal mass-matrix.

We define:

$$U^T = (u, c, t, u', c', t') \quad \text{and} \quad D^T = (d, s, b, d', s', b')$$

such that the coupling of the flavour gauge bosons to the quarks are described by the Lagrangian-part

$$\begin{aligned}\mathcal{L} \supset &+ \bar{U}_i \gamma_\mu (\mathcal{G}_L^u + \mathcal{G}_R^u)_{ij,m} U_j \cdot \chi_m \\ &+ \bar{D}_i \gamma_\mu (\mathcal{G}_L^d + \mathcal{G}_R^d)_{ij,m} D_j \cdot \chi_m\end{aligned}$$

where  $m$  is understood to run from 1 to 24 and the tensors  $\mathcal{G} \equiv \mathcal{G}[C_{L,R}, g_{Q,U,D}]$  can be read off from the couplings of flavour eigenstates  $A_Q$ ,  $A_U$ , and  $A_D$  to the quarks, that are listed below: i.e.

$$(\mathcal{G}_L^u)_{13,1} = \frac{g_Q}{2} c_{uL1} (\lambda_{SU(3)}^1)_{13} c_{uL3}, \quad (\mathcal{G}_R^d)_{42,18} = \frac{g_D}{2} s_{dL1} (\lambda_{SU(3)}^2)_{12} c_{dL2}. \quad (\text{A.3})$$

The rotation to the mass-eigenstates of the heavy gauge bosons redefines the couplings:

$$\begin{aligned}\mathcal{L} \supset &+ \bar{U}_i \gamma_\mu (\hat{\mathcal{G}}_L^u + \hat{\mathcal{G}}_R^u)_{ij,k} U_j \cdot \varphi_k \\ &+ \bar{D}_i \gamma_\mu (\hat{\mathcal{G}}_L^d + \hat{\mathcal{G}}_R^d)_{ij,k} D_j \cdot \varphi_k,\end{aligned}$$

where

$$(\hat{\mathcal{G}}_{L,R}^\alpha)_{ij,m} = \sum_k \mathcal{W}(\varphi_m, \chi_k) (\mathcal{G}_{L,R}^\alpha)_{ij,m}, \quad \text{with} \quad \alpha = u, d. \quad (\text{A.4})$$

Notice that in the rest of the paper we either use  $\{i, j\} \in \{1, \dots, 6\}$  or refer directly to the (SM or exotic) quark flavour: i.e.

$$(\hat{\mathcal{G}}_{L,R}^u)_{15,m} \equiv (\hat{\mathcal{G}}_{L,R}^u)_{uc',m}, \quad (\hat{\mathcal{G}}_{L,R}^d)_{23,m} \equiv (\hat{\mathcal{G}}_{L,R}^d)_{sb,m}. \quad (\text{A.5})$$

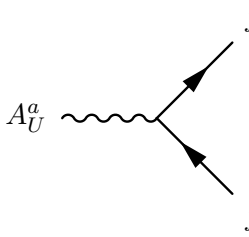
**$A_Q$  coupling**

$$A_Q^a \text{ coupling} \quad \left| \quad \begin{array}{l} \text{with the actual values for } \bar{f}, f \text{ and } C: \\ \text{Diagram: } A_Q^a \text{ wavy line} \rightarrow \begin{array}{l} \nearrow f\text{-bar} \\ \searrow f \end{array} \\ \text{Equation: } = i \frac{g_Q}{2} \gamma_\mu (P_L C_L + P_R C_R) \end{array} \right.$$

$$\begin{aligned}
A_Q^a \bar{u}_i u_j & : C_R = +s_{uRi}(V\lambda_{SU(3)}^a V^\dagger)_{ij}s_{uRj} \\
& : C_L = +c_{uLi}(V\lambda_{SU(3)}^a V^\dagger)_{ij}c_{uLj} \\
A_Q^a \bar{u}'_i u'_j & : C_R = +c_{uRi}(V\lambda_{SU(3)}^a V^\dagger)_{ij}c_{uRj} \\
& : C_L = +s_{uLi}(V\lambda_{SU(3)}^a V^\dagger)_{ij}s_{uLj} \\
A_Q^a \bar{u}_i u'_j & : C_R = -s_{uRi}(V\lambda_{SU(3)}^a V^\dagger)_{ij}c_{uRj} \\
& : C_L = +c_{uLi}(V\lambda_{SU(3)}^a V^\dagger)_{ij}s_{uLj} \\
A_Q^a \bar{u}'_i u_j & : C_R = -c_{uRi}(V\lambda_{SU(3)}^a V^\dagger)_{ij}s_{uRj} \\
& : C_L = +s_{uLi}(V\lambda_{SU(3)}^a V^\dagger)_{ij}c_{uLj}
\end{aligned}$$

$$\begin{aligned}
A_Q^a \bar{d}_i d_j & : C_R = +s_{dRi}(\lambda_{SU(3)}^a)_{ij}s_{dRj} \\
& : C_L = +c_{dLi}(\lambda_{SU(3)}^a)_{ij}c_{dLj} \\
A_Q^a \bar{d}'_i d'_j & : C_R = +c_{dRi}(\lambda_{SU(3)}^a)_{ij}c_{dRj} \\
& : C_L = +s_{dLi}(\lambda_{SU(3)}^a)_{ij}s_{dLj} \\
A_Q^a \bar{d}_i d'_j & : C_R = -s_{dRi}(\lambda_{SU(3)}^a)_{ij}c_{dRj} \\
& : C_L = +c_{dLi}(\lambda_{SU(3)}^a)_{ij}s_{dLj} \\
A_Q^a \bar{d}'_i d_j & : C_R = -c_{dRi}(\lambda_{SU(3)}^a)_{ij}s_{dRj} \\
& : C_L = +s_{dLi}(\lambda_{SU(3)}^a)_{ij}c_{dLj}
\end{aligned}$$

### $A_U$ coupling

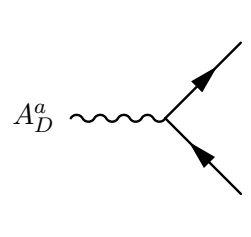


$$= i\frac{g_U}{2}\gamma_\mu(P_L C_L + P_R C_R)$$

with the actual values for  $\bar{f}$ ,  $f$  and  $C$ :

$$\begin{aligned}
A_U^a \bar{u}_i u_j & : C_R = +c_{uRi}(\lambda_{SU(3)}^a)_{ij}c_{uRj} \\
& : C_L = +s_{uLi}(\lambda_{SU(3)}^a)_{ij}s_{uLj} \\
A_U^a \bar{u}'_i u'_j & : C_R = +s_{uRi}(\lambda_{SU(3)}^a)_{ij}s_{uRj} \\
& : C_L = +c_{uLi}(\lambda_{SU(3)}^a)_{ij}c_{uLj} \\
A_U^a \bar{u}_i u'_j & : C_R = +c_{uRi}(\lambda_{SU(3)}^a)_{ij}s_{uRj} \\
& : C_L = -s_{uLi}(\lambda_{SU(3)}^a)_{ij}c_{uLj} \\
A_U^a \bar{u}'_i u_j & : C_R = +s_{uRi}(\lambda_{SU(3)}^a)_{ij}c_{uRj} \\
& : C_L = -c_{uLi}(\lambda_{SU(3)}^a)_{ij}s_{uLj}
\end{aligned}$$

### $A_D$ coupling



$$= i\frac{g_D}{2}\gamma_\mu(P_L C_L + P_R C_R)$$

with the actual values for  $\bar{f}$ ,  $f$  and  $C$ :

$$\begin{aligned}
A_D^a \bar{d}_i d_j & : C_R = +c_{dRi}(\lambda_{SU(3)}^a)_{ij}c_{dRj} \\
& : C_L = +s_{dLi}(\lambda_{SU(3)}^a)_{ij}s_{dLj} \\
A_D^a \bar{d}'_i d'_j & : C_R = +s_{dRi}(\lambda_{SU(3)}^a)_{ij}s_{dRj} \\
& : C_L = +c_{dLi}(\lambda_{SU(3)}^a)_{ij}c_{dLj} \\
A_D^a \bar{d}_i d'_j & : C_R = +c_{dRi}(\lambda_{SU(3)}^a)_{ij}s_{dRj} \\
& : C_L = -s_{dLi}(\lambda_{SU(3)}^a)_{ij}c_{dLj} \\
A_D^a \bar{d}'_i d_j & : C_R = +s_{dRi}(\lambda_{SU(3)}^a)_{ij}c_{dRj} \\
& : C_L = -c_{dLi}(\lambda_{SU(3)}^a)_{ij}s_{dLj}
\end{aligned}$$

## B Couplings of the Lightest Flavour Gauge Boson

As an example, we report in fig. 8 and 9 the couplings of the lightest gauge boson to the light down- and up-type quarks for the exclusive  $V_{ub}$  case and scattering on all the parameters of the model. The colour-coding corresponds to the mass splitting of the lightest to the next-to-lightest flavour gauge boson mass. Namely, red points correspond to large splitting while black points to degeneracy, yellow to intermediate splitting. We observe that the flavour-violating couplings with the last (first) two generations are in general the largest (smallest) ones. This is related to the sequential breaking of the flavour symmetry encoded into hierarchical structure of the flavon VEVs.

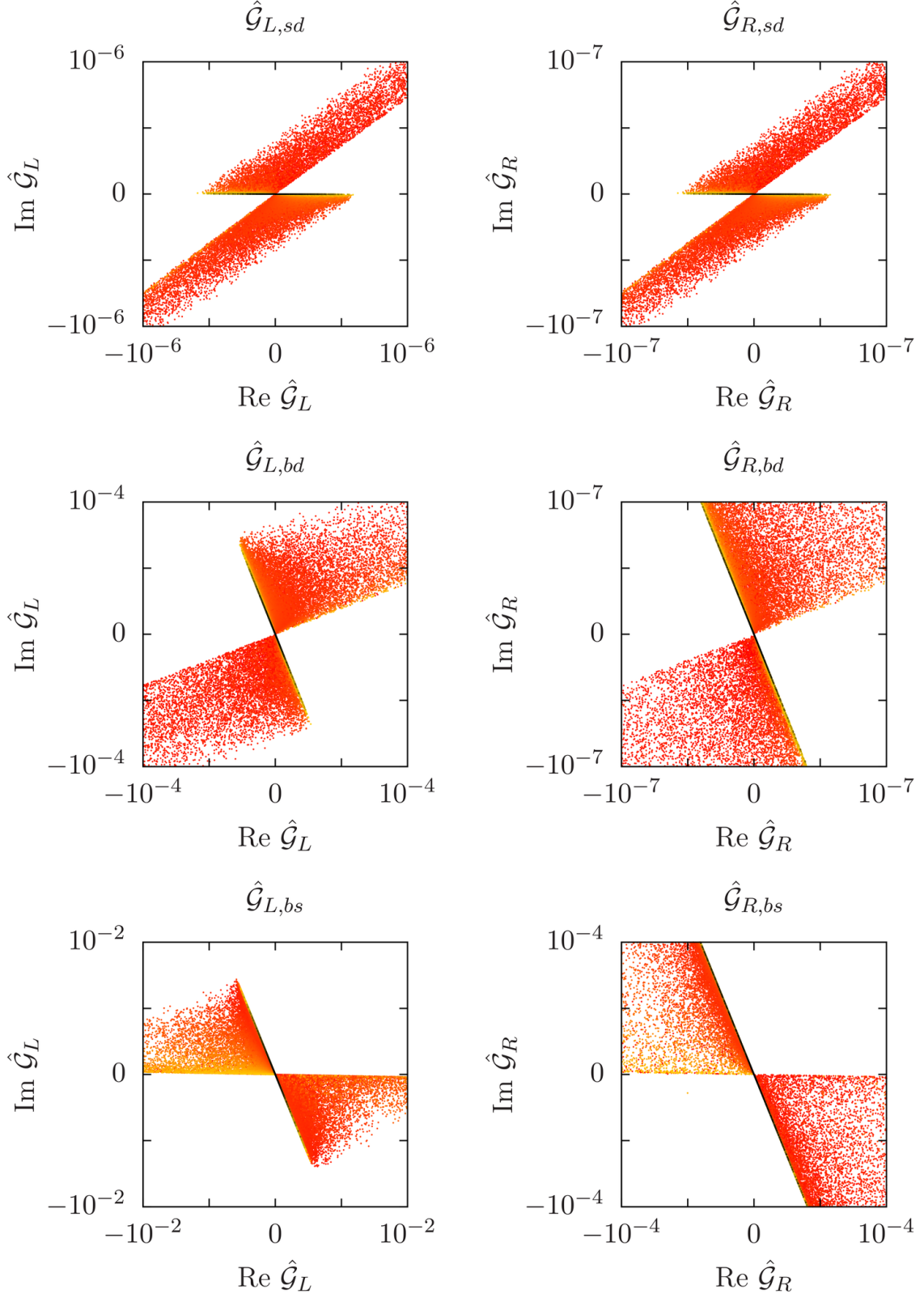


Figure 8: *The couplings of the lightest flavour gauge boson to the down-type SM quarks.*

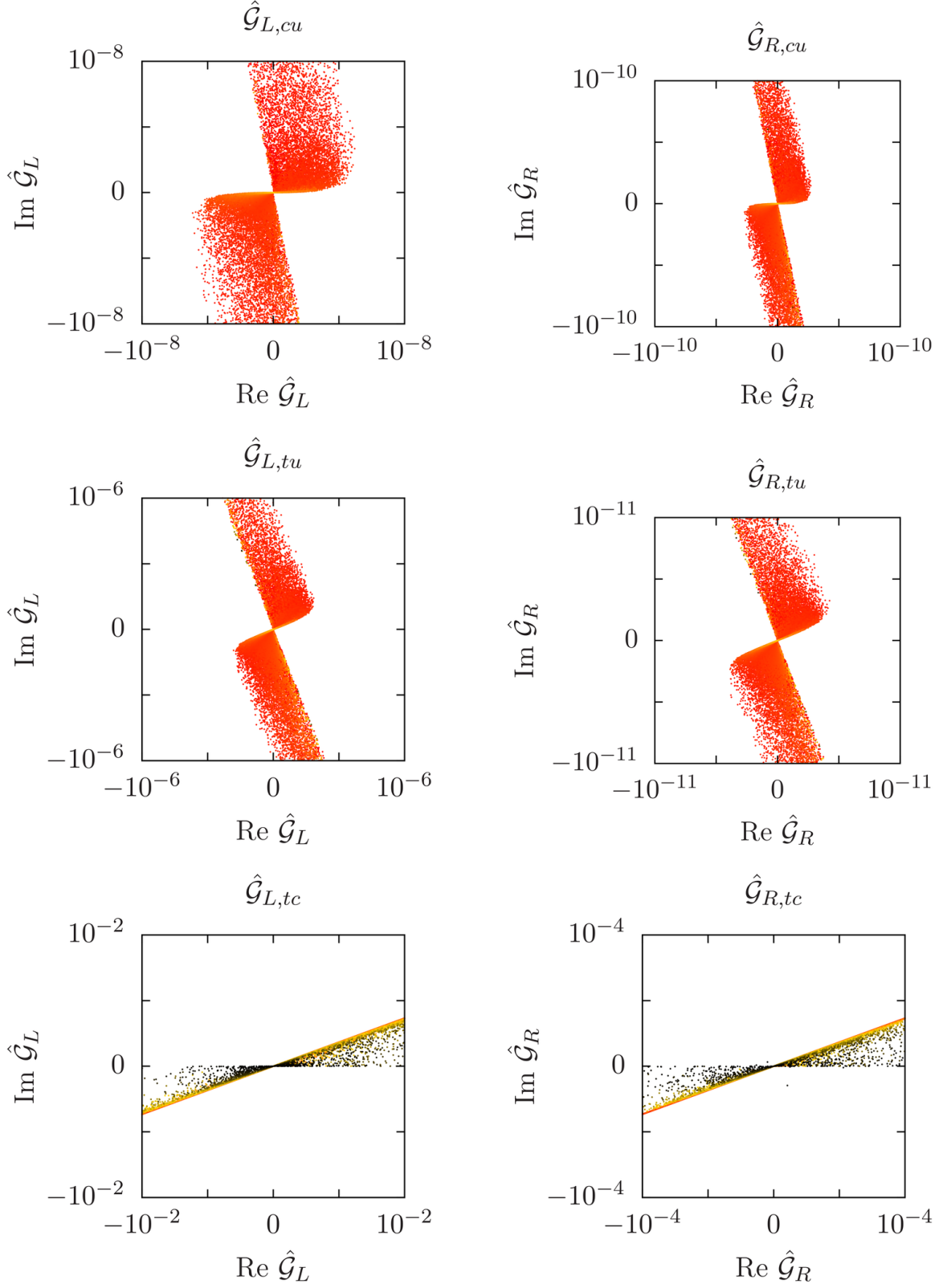


Figure 9: *The couplings of the lightest flavour gauge boson to the up-type SM quarks.*

## References

- [1] F. Feruglio, C. Hagedorn, Y. Lin, and L. Merlo, *Lepton Flavour Violation in a Supersymmetric Model with  $A_4$  Flavour Symmetry*, *Nucl. Phys.* **B832** (2010) 251–288, [arXiv:0911.3874](#).
- [2] L. Merlo, S. Rigolin, and B. Zaldivar, *Flavour Violation in a Supersymmetric  $T'$  Model*, *JHEP* **11** (2011) 047, [arXiv:1108.1795](#).
- [3] R. S. Chivukula and H. Georgi, *Composite Technicolor Standard Model*, *Phys. Lett.* **B188** (1987) 99.
- [4] L. J. Hall and L. Randall, *Weak Scale Effective Supersymmetry*, *Phys. Rev. Lett.* **65** (1990) 2939–2942.
- [5] M. Ciuchini, G. Degrossi, P. Gambino, and G. F. Giudice, *Next-To-Leading (QCD) Corrections to  $\bar{B} \rightarrow X_s \gamma$  in Supersymmetry*, *Nucl. Phys.* **B534** (1998) 3–20, [hep-ph/9806308](#).
- [6] A. J. Buras, P. Gambino, M. Gorbahn, S. Jager, and L. Silvestrini, *Universal Unitarity Triangle and Physics Beyond the Standard Model*, *Phys. Lett.* **B500** (2001) 161–167, [hep-ph/0007085](#).
- [7] G. Isidori, Y. Nir, and G. Perez, *Flavor Physics Constraints for Physics Beyond the Standard Model*, *Ann. Rev. Nucl. Part. Sci.* **60** (2010) 355, [arXiv:1002.0900](#).
- [8] G. D’Ambrosio, G. F. Giudice, G. Isidori, and A. Strumia, *Minimal Flavour Violation: an Effective Field Theory Approach*, *Nucl. Phys.* **B645** (2002) 155–187, [hep-ph/0207036](#).
- [9] V. Cirigliano, B. Grinstein, G. Isidori, and M. B. Wise, *Minimal flavor violation in the lepton sector*, *Nucl. Phys.* **B728** (2005) 121–134, [hep-ph/0507001](#).
- [10] S. Davidson and F. Palorini, *Various Definitions of Minimal Flavour Violation for Leptons*, *Phys. Lett.* **B642** (2006) 72–80, [hep-ph/0607329](#).
- [11] R. Alonso, G. Isidori, L. Merlo, L. A. Munoz, and E. Nardi, *Minimal Flavour Violation Extensions of the Seesaw*, *JHEP* **06** (2011) 037, [arXiv:1103.5461](#).
- [12] B. Grinstein, M. Redi, and G. Villadoro, *Low Scale Flavor Gauge Symmetries*, *JHEP* **11** (2010) 067, [arXiv:1009.2049](#).
- [13] T. Feldmann, *See-Saw Masses for Quarks and Leptons in  $SU(5)$* , *JHEP* **04** (2011) 043, [arXiv:1010.2116](#).
- [14] D. Guadagnoli, R. N. Mohapatra, and I. Sung, *Gauged Flavor Group with Left-Right Symmetry*, *JHEP* **04** (2011) 093, [arXiv:1103.4170](#).
- [15] T. Feldmann, M. Jung, and T. Mannel, *Sequential Flavour Symmetry Breaking*, *Phys. Rev.* **D80** (2009) 033003, [arXiv:0906.1523](#).



- [16] R. Alonso, M. B. Gavela, L. Merlo, and S. Rigolin, *On the Scalar Potential of Minimal Flavour Violation*, *JHEP* **07** (2011) 012, [arXiv:1103.2915](#).
- [17] A. J. Buras, L. Merlo, and E. Stamou, *The Impact of Flavour Changing Neutral Gauge Bosons on  $\bar{B} \rightarrow X_s \gamma$* , [arXiv:1105.5146](#).
- [18] A. J. Buras, M. Misiak, and J. Urban, *Two-Loop QCD Anomalous Dimensions of Flavour-Changing Four-Quark Operators Within and Beyond the Standard Model*, *Nucl. Phys.* **B586** (2000) 397–426, [hep-ph/0005183](#).
- [19] A. J. Buras, S. Jager, and J. Urban, *Master Formulae for  $\Delta_F = 2$  NLO-QCD Factors in the Standard Model and Beyond*, *Nucl. Phys.* **B605** (2001) 600–624, [hep-ph/0102316](#).
- [20] R. Babich *et. al.*,  *$K^0 - \bar{K}^0$  Mixing Beyond the Standard Model and CP-Violating Electroweak Penguins in Quenched QCD with Exact Chiral Symmetry*, *Phys. Rev.* **D74** (2006) 073009, [hep-lat/0605016](#).
- [21] D. Becirevic, V. Gimenez, G. Martinelli, M. Papinutto, and J. Reyes, *B-Parameters of the Complete Set of Matrix Elements of  $\Delta_B = 2$  Operators from the Lattice*, *JHEP* **04** (2002) 025, [hep-lat/0110091](#).
- [22] A. J. Buras and D. Guadagnoli, *Correlations among New CP Violating Effects in  $\Delta F = 2$  Observables*, *Phys. Rev.* **D78** (2008) 033005, [arXiv:0805.3887](#).
- [23] A. J. Buras, D. Guadagnoli, and G. Isidori, *On  $\epsilon_K$  Beyond Lowest Order in the Operator Product Expansion*, *Phys. Lett.* **B688** (2010) 309–313, [arXiv:1002.3612](#).
- [24] **UTfit** Collaboration, M. Bona *et. al.*, *The Ufit Collaboration Report on the Status of the Unitarity Triangle Beyond the Standard Model. I: Model- Independent Analysis and Minimal Flavour Violation*, *JHEP* **03** (2006) 080, [hep-ph/0509219](#).
- [25] **Belle** Collaboration, K. Ikado *et. al.*, *Evidence of the Purely Leptonic Decay  $B^- \rightarrow \tau^- \bar{\nu}_\tau$* , *Phys. Rev. Lett.* **97** (2006) 251802, [hep-ex/0604018](#).
- [26] G. Isidori and P. Paradisi, *Hints of Large  $\tan(\beta)$  in Flavour Physics*, *Phys. Lett.* **B639** (2006) 499–507, [hep-ph/0605012](#).
- [27] **D0** Collaboration, V. M. Abazov *et. al.*, *Measurement of the Anomalous Like-Sign Dimuon Charge Asymmetry with  $9 \text{ Fb}^{-1}$  of  $p\bar{p}$  Collisions*, *Phys. Rev.* **D84** (2011) 052007, [arXiv:1106.6308](#).
- [28] A. Lenz, *Theoretical Status of the CKM Matrix*, [arXiv:1108.1218](#).
- [29] T. Inami and C. S. Lim, *Effects of Superheavy Quarks and Leptons in Low-Energy Weak Processes  $K_L \rightarrow \mu \bar{\mu}$ ,  $K^+ \rightarrow \pi^+ \nu \bar{\nu}$  and  $K^0 \leftrightarrow \bar{K}^0$* , *Prog. Theor. Phys.* **65** (1981) 297.

- [30] E. Lunghi and A. Soni, *Possible Indications of New Physics in  $B(D)$ -Mixing and in  $\sin(2\beta)$  Determinations*, *Phys. Lett.* **B666** (2008) 162–165, [arXiv:0803.4340](#).
- [31] A. J. Buras and D. Guadagnoli, *On the Consistency Between the Observed Amount of CP Violation in the  $K$ - and  $B(D)$ -Systems Within Minimal Flavor Violation*, *Phys. Rev.* **D79** (2009) 053010, [arXiv:0901.2056](#).
- [32] A. Lenz *et. al.*, *Anatomy of New Physics in  $B - \bar{B}$  Mixing*, *Phys. Rev.* **D83** (2011) 036004, [arXiv:1008.1593](#).
- [33] **RBC Collaboration**, D. J. Antonio *et. al.*, *Neutral Kaon Mixing from 2+1 Flavor Domain Wall QCD*, *Phys. Rev. Lett.* **100** (2008) 032001, [hep-ph/0702042](#).
- [34] C. Aubin, J. Laiho, and R. S. Van de Water, *The Neutral kaon mixing parameter  $B(K)$  from unquenched mixed-action lattice QCD*, *Phys.Rev.* **D81** (2010) 014507, [arXiv:0905.3947](#).
- [35] J. Laiho, E. Lunghi, and R. S. Van de Water, *Lattice QCD Inputs to the CKM Unitarity Triangle Analysis*, *Phys. Rev.* 034503, [arXiv:0910.2928](#).
- [36] T. Bae, Y.-C. Jang, C. Jung, H.-J. Kim, J. Kim, *et. al.*,  *$B_K$  using HYP-smearred staggered fermions in  $N_f = 2 + 1$  unquenched QCD*, *Phys.Rev.* **D82** (2010) 114509, [arXiv:1008.5179](#).
- [37] **ETM Collaboration** Collaboration, M. Constantinou *et. al.*,  *$B_K$ -parameter from  $N_f = 2$  twisted mass lattice QCD*, *Phys.Rev.* **D83** (2011) 014505, [arXiv:1009.5606](#).
- [38] Y. Aoki *et. al.*, *Continuum Limit of  $B_K$  from 2+1 Flavor Domain Wall QCD*, *Phys. Rev.* **D84** (2011) 014503, [arXiv:1012.4178](#).
- [39] J. Brod and M. Gorbahn,  *$\epsilon_K$  at Next-To-Next-To-Leading Order: the Charm-Top-Quark Contribution*, *Phys. Rev.* **D82** (2010) 094026, [arXiv:1007.0684](#).
- [40] J. Brod and M. Gorbahn, *The NNLO Charm-Quark Contribution to  $\epsilon_K$  and  $\Delta M_K$* , [arXiv:1108.2036](#).
- [41] E. Lunghi and A. Soni, *Possible Evidence for the Breakdown of the CKM-Paradigm of CP-Violation*, *Phys. Lett.* **B697** (2011) 323–328, [arXiv:1010.6069](#).
- [42] **Particle Data Group** Collaboration, K. Nakamura *et. al.*, *Review of Particle Physics*, *J. Phys.* **G37** (2010) 075021.
- [43] K. G. Chetyrkin *et. al.*, *Charm and Bottom Quark Masses: an Update*, *Phys. Rev.* **D80** (2009) 074010, [arXiv:0907.2110](#).
- [44] A. J. Buras, M. Jamin, and P. H. Weisz, *Leading and Next-To-Leading QCD Corrections to Epsilon Parameter and  $B^0 - \bar{B}^0$  Mixing in the Presence of a Heavy Top Quark*, *Nucl. Phys.* **B347** (1990) 491–536.

- [45] J. Urban, F. Krauss, U. Jentschura, and G. Soff, *Next-To-Leading Order QCD Corrections for the  $B^0 - \bar{B}^0$  Mixing with an Extended Higgs Sector*, *Nucl. Phys.* **B523** (1998) 40–58, [hep-ph/9710245](#).
- [46] C. McNeile, C. T. H. Davies, E. Follana, K. Hornbostel, and G. P. Lepage, *High-Precision  $f_{B_s}$  and HQET from Relativistic Lattice QCD*, [arXiv:1110.4510](#).
- [47] **For the CDF Collaboration**, G. Giurgiu, *New Measurement of the  $B_s$  Mixing Phase at CDF*, *PoS ICHEP2010* (2010) 236, [arXiv:1012.0962](#).
- [48] **D0 Collaboration**, V. M. Abazov *et. al.*, *Measurement of the CP-Violating Phase  $\phi_s^{J/\psi\phi}$  Using the Flavor-Tagged Decay  $B_s^0 \rightarrow J/\psi\phi$  in  $8 \text{ Fb}^{-1}$  of  $p\bar{p}$  Collisions*, [arXiv:1109.3166](#).
- [49] P. Koppenburg, *talk at Physics in Collision 2011, Vancouver, BC, Canada, 28 August-1 September 2011*.
- [50] A. J. Buras, *Minimal Flavour Violation and Beyond: Towards a Flavour Code for Short Distance Dynamics*, *Acta Phys. Polon.* **B41** (2010) 2487–2561, [arXiv:1012.1447](#).
- [51] M. Blanke, A. J. Buras, D. Guadagnoli, and C. Tarantino, *Minimal Flavour Violation Waiting for Precise Measurements of  $\Delta M_s$ ,  $S_{\psi\phi}$ ,  $A_{sl}^s$ ,  $|V_{ub}|$ ,  $\gamma$  and  $B_{s,d}^0 \rightarrow \mu^+\mu^-$* , *JHEP* **10** (2006) 003, [hep-ph/0604057](#).
- [52] A. J. Buras, M. Spranger, and A. Weiler, *The Impact of Universal Extra Dimensions on the Unitarity Triangle and Rare  $K$  and  $B$  Decays*, *Nucl. Phys.* **B660** (2003) 225–268, [hep-ph/0212143](#).
- [53] M. Blanke and A. J. Buras, *Lower Bounds on  $\Delta M_{s,d}$  from Constrained Minimal Flavour Violation*, *JHEP* **05** (2007) 061, [hep-ph/0610037](#).
- [54] A. J. Buras, A. Poschenrieder, M. Spranger, and A. Weiler, *The Impact of Universal Extra Dimensions on  $\bar{B} \rightarrow X_s\gamma$ ,  $\bar{B} \rightarrow X_sg$ ,  $\bar{B}X_s\mu^+\mu^-$ ,  $K_L \rightarrow \pi^0 e^+e^-$ , and  $\epsilon'/\epsilon$* , *Nucl. Phys.* **B678** (2004) 455–490, [hep-ph/0306158](#).
- [55] A. J. Buras, M. V. Carlucci, S. Gori, and G. Isidori, *Higgs-Mediated FCNCs: Natural Flavour Conservation Vs. Minimal Flavour Violation*, *JHEP* **10** (2010) 009, [arXiv:1005.5310](#).
- [56] M. Blanke, A. J. Buras, K. Gemmler, and T. Heidsieck,  *$\Delta F = 2$  Observables and  $\bar{B} \rightarrow X_Q\gamma$  Decays in the Left-Right Asymmetric Model: Higgs Particles Striking Back*, [arXiv:1111.5014](#).